藥學博士學位論文

Role of Ubiquitin-specific Protease 47 in Hypoxia-induced Epithelial Mesenchymal Transition in Human Colorectal Cancer Cells

저산소 상태에 의해 유도된 대장암 세포의 상피간엽이행 촉진 과정에서 USP47 의 역할

2018 年 2 月

서울大學校 大學院

藥學科 醫藥生命科學專攻

藥學博士學位論文

Role of Ubiquitin-specific Protease 47 in Hypoxia-induced Epithelial Mesenchymal Transition in Human Colorectal Cancer Cells

저산소 상태에 의해 유도된 대장암 세포의 상피간엽이행 촉진 과정에서 USP47의 역할

指導敎授 徐 榮 俊

이 論文을 藥學博士學位論文으로 提出함

2017年 6月

서울大學校 大學院

藥學科 醫藥生物化學 專攻

崔 倍 正

崔 倍 正의 藥學博士學位論文을 認准함

2017年 6月

委 員 長 정 규 원 印

副委員長 이 정 원 印

委 員 서 영 준 印

委 員 한 병 우 印

委 員 나 혜 경 印

Role of Ubiquitin-specific Protease 47

in Hypoxia-induced Epithelial Mesenchymal Transition

in Human Colorectal Cancer Cells

by

Bae-Jung Choi

A thesis submitted in partial fulfillment of the requirements
for the degree of

DOCTOR OF PHILOSOPHY
(Pharmacy: Pharmaceutical bioscience major)

under the supervision of Professor Young-Joon Surh

at the
College of Pharmacy,
Seoul National University

February 2018

Abstract

Ubiquitin is a highly conserved regulatory protein that is abundant in all types of cells and regulates diverse cellular processes by virtue of its attachment to target proteins. Most eukaryotic organisms use ubiquitin as a versatile tool to control a wide variety of proteins' stability, intracellular localization, transcriptional regulation, endocytosis, lysosomal transport and kinase signaling. The ubiquitin-dependent system, therefore, guides various target proteins to degradation or other ubiquitin-related pathways, thereby regulating most cellular responses.

Ubiquitin-dependent processes are reversible and countered by deubiquitinating enzymes (DUBs). DUBs are a large group of proteases that regulate ubiquitin processes by recognizing specific proteins that have been conjugated to mono- or poly- ubiquitin. Through highly selective recognition

of specific substrates, DUBs can cleave the peptide or iso-peptide bond between ubiquitin or ubiquitin-like gene products and substrate proteins more precisely than lysosomal degradation or other proteolytic mechanisms. Various research groups have noted that DUBs that precisely regulate specific ubiquitin-dependent cellular pathways could be therapeutic targets for various disease, including cancer progression.

Epithelial-mesenchymal transition (EMT), which involves the dissolution of cadherin-mediated cell-cell adhesion and a dramatic re-organization of the cytoskeleton with a resulting acquisition of migratory and invasive capabilities, occurs during the metastatic phase of cancer progression. In most tumors, EMT is accompanied by hypoxia. In this study, a novel role of ubiquitin-specific protease 47 (USP47) was identified as a potential mediator of the epithelial-mesenchymal transition (EMT) under hypoxic conditions.

Immunofluorescence staining of human colorectal tissue microarrays revealed that USP47 is overexpressed in colorectal adenocarcinoma tissues compared with normal adjacent tissues. However, the intracellular signaling molecule that mediates hypoxia-induced EMT remained overlooked. The expression of USP47 was found to be elevated in three different human colorectal cancer cell lines. The enhancement of USP47 in colorectal cancer cells under hypoxic conditions induced the disassembly of E-cadherin and promoted EMT through deubiquitination of Snail. Silencing of USP47 accelerated the proteasomal degradation of Snail and inhibited EMT. Notably, hypoxia-induced USP47 upregulation was mediated by Sox9. These results demonstrate, for the first time, the role for USP47, as a novel target of Sox9, in the regulation of EMT and the metastasis of colorectal cancer cells.

Table of Contents

List of Figures

List of Tables

List of Abbreviations

BAP-1	BRCA associated protein-1
CRC	Colorectal Cancer
CYLD	Cylindromatosis
DUB	Deubiquitinating enzymes
EMT	Epithelial-Mesenchymal Transition
EGFR	Epidermal growth factor receptor
E1	Ubiquitin activating enzyme
E2	Ubiquitin conjugate enzyme
E3	Ubiquitin ligase
GAPDH	Glyceraldehyde phosphate-3 dehydrogenase
HIF	Hypoxia-inducible factor
HRE	Hypoxia response element
NF-κB	Nuclear factor - kappa B
POL-β	DNA polymerase beta
RMA	Rectal mucinous adenocarcinoma

SNAG	Snail1/GFI
TGF-β	Tumor growth factor - β
USP	Ubiquitin-specific protease family
USP47	Ubiquitin-specific protease 47
UCH	Ubiquitin C-terminal hydrolases (UCHs),
MJD	Machado-Josephin domain proteases
OUT	Ovarian tumor proteases domains
JAMM	Jab1/Mov34/Mpr1 Pad1 N-terminal+ (MPN+) (JAMM) domain proteases

Introduction

1. Role of ubiquitin in cellular processes

In 1975, Gedion Goldstein discovered a regulatory protein that consists of 76 amino acids and is present in most living cells. The protein, named ubiquitin, was further characterized throughout the 1970s and 1980s. Ubiquitin functions by being conjugated to multiple substrate proteins. The attachment of ubiquitins to these substrate proteins, termed ubiquitination, occurs through peptide or isopeptide bond formation between a glycine residue at its C-terminus of ubiquitin and 7 lysine residues (Lys^{6}, Lys^{11}, Lys^{27}, Lys^{29}, Lys^{33}, and Lys^{48}) in the substrate protein. Ubiquitination occurs in sequential stages of activation, conjugation and ligation catalyzed by three different proteins; ubiquitin activating enzyme (E1), ubiquitin-conjugating enzyme (E2) and ubiquitin ligase (E3), respectively. As illustrated in Figure

1, E1 activates ubiquitin using ATP, and E2 enzymes form thiol esters to transfer ATP energy to E3, which then attaches ubiquitin to substrate proteins (Pickart et al., 2004; Komander, et al., 2012). Eukaryotic cells use ubiquitination to mark substrate proteins for proteasomal degradation, and to coordinate the cellular localization of proteins, control the activation of proteins and modulate protein-protein interactions. Ubiquitin-related pathways are a ATP-dependent, reversible process maintained by E1, E2 and E3 enzymatic reactions. Significant progress in the understanding of ubiquitin-conjugation and its role in regulating protein degradation and cellular signaling pathways has been made since the discovery of ubiquitin. However, de-conjugation of ubiquitin has not yet been completely elucidated.

2. General properties of deubiquitinating enzymes (DUBs)

DUBs are a large group of cysteine proteases that can reverse ubiquitin pathways. The primary function of DUBs is the cleavage of mono- or poly-ubiquitin chains from substrate proteins. Ubiquitination is a post-translational modification where single- or multiple ubiquitin chains are attached to lysine residues of a substrate protein. Ubiquitin is encoded by the UBA52, RPS27A, UBB and UBC genes in mammals. The UBA52 and RPS27A genes produce ubiquitin that is fused to ribosomal proteins and the UBB and UBC genes produce polyubiquitin (Nijman, et al., 2005, Pickart, et al., 1985). DUBs cleave the ubiquitin from these proteins and produce active ubiquitin monomers. DUBs also cleave ubiquitin monomers whose C-terminal tails have accidentally been attached to small cellular nucleophiles (Hicke, *et al.*, 2001). These small ubiquitin-amides and ubiquitin-thioesters may be formed during standard ubiquitination reactions of the E1-E2-E3 cascade by nucleophilic attacks on the thioester bonds between ubiquitin and

these enzymes. Ubiquitin C-terminal hydrolase is an example of a DUB that hydrolyzes these bonds with broad specificity (Wilborg, et al, 1985, Wilkinson, et al, 1995). Free polyubiquitin chains are also cleaved by DUBs to produce monoubiquitin. The chains can be produced by the E1-E2-E3 machinery within the cell in the absence of any substrate protein. Another source of free polyubiquitin include the products of ubiquitin-substrate cleavage. If DUBs cleave the base of a polyubiquitin chain attached to a protein, then the entire chain will be released and needs to be recycled by other DUBs (Hicke, et al. 2001). As illustrated in Figure 2, DUBs play the antagonistic role in this axis by removing these ubiquitin chains and thereby reversing the instability of the proteins to which they are attached (Reyes-Turcu, et al., 2009).

Although cellular details of their substrate specificity and regulation are not completely revealed yet, considerable progress has been made in the

understanding of enzymatic mechanisms of DUBs. Quantitative studies on activity and protein-protein interactions led to new insights into the functions of human DUBs.

2. 1. Subfamilies of DUBs

There are 102 identified DUB genes in humans that can be classified into 5 subfamilies. The cysteine proteases comprise ubiquitin C-terminal hydrolases (UCHs), ubiquitin-specific proteases (USPs), ovarian tumor protease (OTU) domains and Machado-Josephin domain proteases (MJDs). The metalloprotease group contains only the Jab1/Mov34/Mpr1, Pad1, N-terminal+ (MPN+; JAMM) domain proteases (Figure 3).

2. 1. 1. The ubiquitin C-terminal hydrolase (UCH) domain

There are four UCH domain deubiquitinating enzymes; UCH-L1, UCH-L3, UCH-L5 and BAP1 (Figure 3). The catalytic core of this family in humans

consists of a 230-amino acid domain (Navarro, et al., 2013). UCH-L1 and UCH-L3 only contain the globular UCH fold, but UCH-L5 contains 100-additional amino acids involved in trimming polyubiquitin from protein degradation at the C-terminal extension. BAP1 possess an additional 500 amino acids containing a nuclear localization signal and a binding site for interaction with BRCA1 in breast cancer (Kulich, et al., 2008, Ventii, et al., 2008, Jensen, et al., 1998, Reyes-Turcu, et al., 2009).

2. 1. 2. The ubiquitin specific protease (USP) domain

Recent studies have shown that the DUBs of USP family consists of 53 different genes. The USPs have 3 subdomains; the finger, palm and thumb, which together resemble a right hand. Although CYLD lacks a finger subdomain, USP domains are highly conserved in the most types of cells (Amerik, et al., 2004, Hu, et al, 2005).

2. 1. 3. The ovarian tumor (OTU) domain

The ovarian tumor (OTU) domain family of DUBs in humans contains 15 OUT domain DUBs, but only half of these have been studied extensively (Marcus, et al, 2011). OUT domain DUBs were identified based on their homology to the ovarian tumor gene involved in the development of ovaries in fruit files. Subsequent studies have demonstrated that several OTU domain DUBs have deubiquitinating activity (Messick, et al., 2008). Recent structural studies indicate that the OTU core domain is composed of five β strands sandwiched between helical domain that varies in the size (Maxim, et al, 2003).

2. 1. 4. Machado-Josephin Domain (MJD) proteases

The Machado-Josephin domain protein Ataxin-3, which has been implicated in the neurodegenerative disorder spinocerebellar ataxia type 3, is the best-studied member of the four human Josephine family proteins (Nicastro, et al., 2005). The structure of the Ataxin-3 Josephin domain was solved by NMR and the overall folds resemble that of the UCH family. (Reyes-Turcu, et al., 2009). K64-linked chain is major target of the active residue of Ataxin-3 (Wolberger, et al., 2014).

2. 1. 5. The JAB1/MPN/Mov34 metalloenzyme (JAMM) domain

The JAMM domain is a highly conserved amino acid. It has been reported that four different types of JAMM domain exist in DUBs (Zhu, et al, 2007). Three of them play a major role at key regulatory points in ubiquitinaing substrates (Yao, et al., 2002). JAMM domain in CSN5 in the COP9

signalosome acts on proteins modified with the ubiquitin-like protein Nedd8 (Cope, et al., 2002).

3. DUBs and cancer

Many research groups have noted that DUBs could be a therapeutic target for specific ubiquitin-related biological processes, including cancer progression. Recent studies independently discovered that DUBs regulate cancer-related processes through interaction with various proteins such as nuclear factor κ-light-chain-enhancer of activated B (NF-κB), hypoxia-inducible factor-1α (HIF-1α) and transforming growth factor-β (TGF-β) (Chen, et al., 2005; Wicks, et al., 2006; Altun, et al., 2012). In this section, I summarize the known functions of DUBs, their substrate targets in cancer progression and therapeutic potential (Table1).

It is well known that HIF-1α protein is rapidly degraded by the ubiquitin system. Ubiquitin C-terminal hydrolase-L1 (UCHL1) directly interacts with Hif-1α and promotes its transcriptional activity in breast cancer cells [Nakashima, et al., 2017] In addition, UCHL1 stabilizes protein kinase B 2 (Akt2) to promote phosphorylation of Akt. Thus, UCHL1 enhances the invasiveness of breast cancer cells (Luo, et al, 2018). A recent study revealed that expression of UCH-L3 inhibits invasion and metastasis and decreases the expression level of epithelial mesenchymal transition (EMT) markers (Song, et al, 2014). However, the role of UCH-L3 in carcinogenesis has been largely unknown [Song, et al., 2014]. BRCA associated protein-1 (BAP1 or UCHL2) has been studied extensively since it was discovered at 1998 (Jensen, et al., 1998). Many research groups independently demonstrated that BAP1 can interact with various proteins, including AHCYL2, ANAPC7, ANKRD17, ASXL1, ASXL2, BRCA1, CBX1, CBX3, EIF4EBP3, FOXK1, FOXK2,

HAT1, HCFC1, HIST2H2AC, HSPA2, IPO4, IPO5, KDM1B, OGT, PPM1G, PSME3, RBBP7 and UBE2O (Sowa, et al., 2009). BAP1 binds directly to BRCA1, but not to BRCA2, to regulate cell growth (Jensen, et al., 1998). BRCA1 also interacts with Host cell factor C1 (HCFC1) in order to associate with chromatin-modifying complexes during cell cycle progression (Misaghi, et al., 2009). Somatic BAP1 mutations are frequently found in uveal melanoma (UVM) biopsies, but detailed mechanisms have, to date, not been clearly identified (Harbour, et al., 2010). Fanconi complementation group D2 (FNACD2) is known to be associated with Fanoni anemia, a recessive genetic disease that can cause cancer. it also has been shown that usp1 is essential for hydrolysis of ubiquitin from mono-ubiquitinated FNACD2 in DNA damage signaling pathways (Nijman, et al.; Wang, et al., 2007). Another study has revealed that USP1 requires USP1 associated factor 1 (UAF1) to exert full deubiquitinating activity, and also regulates FANCD2. Thus, the USP1/UAF1

complex can mediates DNA damage repair in cancer cells (Liang, et al., 2014). In addition, UAF1 can also form a complex with USP12, thereby acting as an activator of USP1 (Dharahar, et al, 2016). USP2a, also known as USP2-69, functions in prostate cancer and it deubiquitinates and stabilizes fatty acid synthase (Graner, et al, 2004). Furthermore, USP2a expression was found to increase during migration and invasion of triple negative breast cancer cell lines (Qu, et al., 2015). Further research has shown that USP2 regulates cell death by targeting of RIP to activate tumor necrosis associated-factor 2 (TRAF2) proteins, and MYC in tumor necrosis factor (TNF) pathways (Mahul-melier, et al, 2012). It has also been reported that Mdm2 is directly regulated by USP2, which results in a suppression of p53 (Wei, et al, 2016). USP2a also regulates epidermal growth factor receptor (EGFR) via a receptor tyrosine kinase protein cascade (Liu, et al., 2013). It has been reported that USP3 negatively regulates BRCA1, which is mutated in familial forms of

breast and ovarian cancer and is involved in double stranded break repair of DNA damage (Sharma, et al., 2014). In another study, USP3 in rat hepatoma suppressed glutathione *S*-transferase A2 (GSTA2) transcription [Whalen, et al, 2006].

The stability of p53 tumor suppressor protein is regulated by the ubiquitin ligase Mdm2. A functional study of USP5 showed that its suppression results in accumulation of unanchored poly-ubiquitins, which compete with ubiquitinated p53 for proteasomal degradation. Thus, down-regulation of USP5 can activate of p53 (Dayal, et al.; 2009, Sparks, et al.; 2014), and increased USP5 has been associated with progression of pancreatic cancer via regulation of FoxM1 protein (Li, et al., 2017). Usp6 (also known as Tre17) has been identified as an oncogene in Ewing's sarcoma (Oliveira, et al., 2014). In addition, aneurysmal bone cysts can be associated with chromosomal rearrangements of USP6 (Oliveira, et al, 2004). Moreover,

up-regulation of USP6 interfered proteasomal degradation of the Wnt receptor Frizzled (Fzd) and enhanced cellular sensitivity to Wnt signals (Babita, et al, 2016). USP6 increases translational activation of the Wnt/β-catenin pathway, though its target substrate has not yet been identified (Madan, et al., 2016). USP6 is also involved in cell cycle regulation and endosomal membrane trafficking through interaction with cell cycle promoting proteins such as TBC (Tre-2/Bub2/Cdc16) family (Funakoshi, et al., 2014). USP7 (HAUSP) is most commonly known as Mdm2 specific DUB. A previous study has revealed that p53 is deubiquitinated by USP7, which promotes tumor suppression (Li, et al., 2002). Expression levels of p53 are regulated by a Mdm2-mediated ubiquitination system; USP7 however, stabilizes p53 when DNA is damaged. Another study also demonstrated that the function of USP7 is related to oncogenic stabilization of p53. Myc and E1A activate p53 through a p19 alternative reading frame (P19ARF) and

USP7 is negatively regulated by P19ARF (Atanassov, et al., 2011). USP8 (known as UBPY) is one of the 20S proteasome subunits comprised of Mcc1, RRM1 and Ckap5, and it regulates cell growth and proliferation (Jeong, 2015). In addition, USP8 plays mainly in the regulation of endosomal trafficking through intracellular signaling proteins such as Hrs-binding protein (Hbp) and STAM via stabilization of epidermal growth factor receptor (EGFR; Berlin2, et al., 2010). USP8 is essential in promoting EGFR degradation through its deubiquitination (Alwan, et al., 2007). During interphase, USP8 deubiquitinating activity is inhibited by interaction with 14-3-3 protein, which is a conserved regulatory molecule related to a multitude of functionally diverse signaling proteins, including kinases, phosphatases, and transmembrane receptors. But its enzymatic function is restored during mitosis after the dissociation of USP8 and 14-3-3, which binds a multitude of functionally diverse signaling proteins, including kinases, phosphatases, and

transmembrane receptors complex (Balif, et al. 2006). Moreover, USP8 regulates the stability of FLIPS as a tumor necrosis factor-related apoptosis-inducing ligand (TRAIL) regulator, and it is related to the PETN-Akt-AIP4 signal pathway (Panner, et al., 2010). A recent study showed that ErbB2 is also regulated by USP8, which maintains basal levels of HIF-1α counteracting von hippel-lindau tumor suppressor (VHL)-mediated ubiquitination (Troilo, et al., 2013).

USP15 play a critical role in cancer cell survival by regulating p53. USP15 directly binds to Mdm2 in cancer cells and stabilizes it. Consequently, Mdm2 negatively regulates p53 and NFATc2, a T cell activator (Zou, et al., 2014). It has also been reported that USP15 interacts with COP signalosome 9 (CSN9) to stabilize IκB-α and so regulate its activation (Schweitzer, et al., 2007). In TGF-β signal pathways, USP15 is a key component of the Smad7-SMAD specific E3 ubiquitin protein ligase 2 (Smurf2). USP15 catalyzes

deubiquitination of TGF-type I receptor (TRI) to regulate mono-ubiquitination of TRI (Eichhorn, et al., 2012). USP15 can also deubiquitinate poly- ubiquitins of Smad2 (Iyengar, et al., 2015). USP19 increases stability of HIF-1α by harboring the PAS and bHLH domains of HIF-1α (Altun, et al., 2012). It has also been also reported that the Kip1 ubiquitination-promoting complex 1 (KPC1), a p27-specific E3 ubiquitin ligase, is stabilized by USP19 (Lu, et al., 2009). USP19 mediates TNF-induced apoptosis by regulating the stability of the inhibitors of apoptosis (IAPs)-1 and -2 (Mei, et al., 2011). In addition, muscle RNG finger 1 (MuRF1) and muscle atrophy F-box (MAFbx/atrogin-1) interact with USP19 in patients with lung or gastrointestinal cancer, but the details of these mechanisms are not yet clear (Bedard, et al, 2015). USP20 was identified as a DUBS of a component of an E3 ubiquitin ligase complex, VHL (pVHL) protein (Kondo, et al., 2000). pVHL ubiquitinates HIF-1α under normoxic conditions, but USP20

deubiquitinates HIF-1α and modulates the expression of hypoxia response element (HRE) and the VEGF gene (Li, et al., 2005). USP20 is associated with NF-κB signaling induction through TRAF6 and Tax protein deubiquitination (Jean-Charles, et al., 2016). USP20 is also known to interact with thyronine deiodinase type 2 (D2), an enzyme that converts thyroxine (T4) to active 3,5,3'-triiodothyronine (T3) (Curcio-Morelli, et al., 2003). It has been reported that USP28 has the potential to regulate cell growth in non-small lung cancers (Lei, et al., 2015). Another study showed that USP28 associates with an F box protein, FBW7a, to regulate MYC stability (Popov, et al., 2007). Moreover, USP28 regulates CHk2 and 53BP1 in an ataxia-telangiectasia mutated under conditions of DNA damage (Zhang, et al., 2006). The far upstream element binding protein (FBP) upregulates Usp29 gene expression, and the resulting USP29 protein product directly binds to p53 and induces apoptosis in response to oxidative stress (Liu, et al., 2011). USP31 is

known to inhibit NF-κB signaling through lysine-63-linked polyubiquitin chains of TRAF2. Additionally, an isoform of USP31, USP31S1 interacts with to p65/RelA (Tzimas, et al., cell signaling, 2006). As mentioned earlier, USP33 (known as VDU1) is an isoform of USP20 and these two proteins interact with pVHL, HIF-1α and 2AR (Li, et al., 2002). In addition, USP33 antagonizes the ubiquitination of β-arrestin and induces seven-transmembrane receptor (7TMR) trafficking, thereby promoting tumor angiogenesis and progression through multiple signal pathways, such as TGF-β and EGFR [Erin, et al., 2013]. USP42 is one of p53-interacting DUBs, such as USP5, USP7 and USP29, that are active during DNA damage response (Hock, et al., 2011). USP46 also binds to the PH domain of leucine-rich-repeats protein phosphatase (PHLPP) and cleaves poly-ubiquitin chains. PHLPP decreases Akt signaling and inhibits proliferation and tumorigenesis of colon cancer cells through USP46-mediated stabilization, (Li, et al., 2013).

USP47 has been shown to interact with Skp1/Cul1/F-box protein - transducing repeat containing protein (SCF-TRCP) to regulate cell survival (Shi, et al., 2015). USP47 also deubiquitinates DNA polymerase during DNA base excision repair (BER) (Peschiaroli, et al., 2009). CYLD is known as a negative regulator of the NF-κB signaling pathway. CYLD interferes with ubiquitination of TNF receptor-associated factor2 (TRAF2), by binding NF-κB essential modulator (NEMO) (Kovalenko, et al., 2003). Moreover, RAF6 and TRAF7 have also been found to be deubiquitinated by CYLD (Yoshida, et al., 2005; Jono, et al., 2004). The phosphatase and tensin homolog (PTEN), an antagonist of the phosphatidylinositol-3-kinase (PI3K) pathways, is a well a known tumor suppressor. A deletion of Ataxin 3 (ATXN3) in lung cancer cells rapidly degrades PTEN, suggesting that ATXN3 may directly deubiquitinate PTEN. Recent studies have shown that mutant ATXN3 causes p53-mediated cell death by regulating the expression of the BAX or PUMA

genes. However, the mechanism by which mutant ATXN3 activates p53-dependent pro-apoptotic signaling pathways remains unknown (Gao, et al., 2015). The expression of ATXN3L increases cell proliferation in breast cancer through deubiquitination of KLF5 (Krueppel-like factor 5), a transcription factor of EGF response elements (Ge, et al., 2015). Research groups have reported that OTUB1 binding to the forkhead transcription factor FOXM1, a key regulator of DNA damage responses and genotoxic drug resistance, by degenerating lys-48-linked ubiquitin-chain. By targeting FOXM1, OTUB1 can enhance proliferation and resistance to drug such as epirubicin in breast and ovarian cancer. (Karunarathna, et al., 2015; Wang, et al., 2016). In addition, overexpression of OTUB1 has been observed in localized prostate cancer tumors and colorectal cancer tissues. The expression level of OTUB1 was associated with promotion of EMT and cancer prognosis in colorectal cancer cells. Another study revealed that the expression level of p53 is

regulated by deubiquitylation of RhoA by OTUB1. (Iglesias-Gato, et al., 2015; Zhou, et al., 2014). Furthermore, OTUB1 deubiquitinates mono- and di-ubiquitinated RAS, resulting in its sequestration on the plasma membrane. Wild-type K-Ras is associated with phosphorylation of the ERK pathway. Histopathological analysis showed that the overexpression of OTUB1 is commonly observed in non-small-cell lung carcinomas, and this result indicates that OTUB1 can be a key regulator of the K-Ras-ERK signaling axis (Baietti, et al., 2016).

In conclusion, there has been accumulating experimental evidence that DUBs have the potential to influence multiple processes in cancer development or progression by affecting ubiquitination or proteasomal degradation of key signaling molecules, including those involved in regulating apoptosis, proliferation, growth regulation, DNA damage responses, hypoxia or oxidative stress responses and signal transduction. In

this dissertation, I explored a novel role for DUBs in hypoxia-induced EMT in colorectal cancer cells.

4. Role of USP47 in hypoxia-induced EMT in human colorectal cancer cells

Colorectal cancer (CRC) is the third most common cancer in men and the second most common cancer in women worldwide (Stewart et al., 2014). Approximately, 1.4 million new cases of CRC are diagnosed each year (Ferlay et al., 2015). The 5-year relative survival rate for patients with stage I, II and III CRC is greater than 70%. However, patients with metastatic stage IV CRC have an overall 5-year survival rate of only about 15% (SEER*Explorer). Metastasis is an extremely inefficient process, and only a small fraction of cells from the tumor mass eventually survive in hypoxic conditions and grow at distant sites (Eccles et al., 2007; Weiss et al., 1990).

During metastasis, tumor cells lose their cell-cell adhesion capacity and acquire the capability of cell motility for invasion through the epithelial-mesenchymal transition (EMT; Gout et al., 2008; Yilmaz et al., 2009). Multiple conditions and factors have been shown to promote EMT [Finger et al., 2010] Hypoxia is known to play a crucial role in inducing EMT by activating HIFs, which regulate distinct signal transduction pathways (Bao et al., 2012). However, the precise molecular events or molecules involved in hypoxia-induced EMT are still largely unresolved.

Among the several other transcription factors that regulate EMT, the zinc-finger transcription factor, Snail plays a fundamental role in hypoxia-induced EMT. Snail suppresses E-cadherin transcription by binding to the E-box site in the E-cadherin promoter under hypoxic conditions in ovarian carcinoma cells (Imai et al., 2003). It has been reported that Snail-induced EMT accelerates metastasis through induction of immune suppression (Kudo-Saito

et al., 2009). Moreover, the overexpression of Snail is associated with poor prognosis in CRC (Kim et al., 2014).

For precise diagnosis and efficient therapeutic intervention of CRC, reliable molecular biomarkers and novel targets need to be identified. To this end, I aimed to explore a crucial intracellular signaling molecule that could mediate hypoxia-induced EMT in CRC. I utilized the microarray database system of the Cancer Genome Atlas and identified the USP47 that belongs to a member of the cysteine protease family of DUBs (Figure 4) (Wilkinson et al., 1997). USP47 is known to regulate DNA repair via deubiquitination of mono-ubiquitinated DNA polymerase β (POL-β) (Peschiaroli et al., 2010), which is commonly mutated in many human tumors (Iwanawa et al., 1999; Wang et al., 1992; Bhattacharyya et al., 1999). USP47 also augments Wnt signaling through deubiquitination of β-catenin in A549 lung and PC3 prostate cancer cells (Shi et al., 2015). However, the involvement of this DUB

in EMT has not yet been demonstrated. Here, I report that upregulation of USP47 under hypoxic conditions stimulates EMT in CRC cells and subsequently their metastatic potential.

Materials and Methods

Datasets and Oncomine® platform bioinformatics

The function of Oncomine® platform (www.oncomine.org) was utilized to locate microarray studies focusing on expression of USP47 in colorectal cancer tissues. The default parameters were used for the USP47 expression analysis (threshold fold change greater or equal to 1.5X, *p* value greater or equal to 1E-4 and gene rank in the tio 10 %). Data analysis was performed as fold change comparing normal tissue with various cancer samples. Gene lists based on fold change and *p* value were obtained from Oncomine® platform datasets. Results were sorted based on the *p* value and then the log-transformed median counted raw data were downloaded from Oncomine® platform.

Cell culture and culture conditions

CCD 841 CoN human normal colon cells and DLD-1, HCT-116, and HT-29 human CRC cells were obtained from American Type Culture Collection (ATCC, Manassas, VA, USA) and cultured in Rosewell Park Memorial Institute (RPMI) 1640 medium, Dulbecco's modified Eagle medium (DMEM), or Mccoy's 5a modified medium supplemented with 10% v/v heat-inactivated horse serum (Gibco). Cells were grown at 37°C in a humidified atmosphere of 5% CO_2. When necessary, cells were exposed to hypoxia (1% O_2) by incubation at 37°C in a 5% CO_2/94% N_2 hypoxia chamber (Forma Scientific).

RNA isolation, quantitative polymerase chain reaction (PCR), and real-time PCR

Total RNA was extracted from CRC cells using TRIzol reagent (Invitrogen, Carlsbad, CA, USA). Total RNA was used for cDNA synthesis with M-MLV reverse transcriptase (Promega, Madison, WI, USA). The cDNA was

PCR amplified with the appropriate primer pairs (Table 1). PCR products were analyzed with RedSafe Nucleic Acid Staining Solution (Intron Biotechnology) for visualization. Real-time PCR was carried out using a RealHelix qRT-PCR Kit (NanoHelix, Korea).

Western blot analysis

Cell and tumor lysates were subjected to electrophoresis on 8–10% sodium dodecyl sulfate (SDS)-polyacrylamide gels and transferred to polyvinylidene difluoride membranes (Pall Corporation). Then, the membranes were incubated with primary antibodies against USP47, vimentin, N-cadherin, Snail, Sox9, β-actin (Santa Cruz Biotechnology, Santa Cruz, CA, USA), E-cadherin (BD Bioscience), or ubiquitin (Cell Signaling Technology, Danvers, MA, USA). Membranes were incubated with horseradish peroxidase-conjugated secondary antibodies (Cell Signaling Technology). Protein blots were visualized with an enhanced chemiluminescence detection kit.

Gene depletion

USP47, Sox9 genes were silenced using *accuTarget*^{tm} predesigned siRNA (Bioneer Inc, Daejeon, Korea): USP47 (1161072); Sox9 (1142996); Negative Control siRNA (SN-1002). Lipofectamine RNA iMAX (Invitrogen, Paisley, UK) was used to cell transfection with 10 nM of each siRNA.

Lentiviral production and infection

Lentiviruses were produced by transfecting HEK-293T cells using lentiviral vectors. HEK-293T cells were transfected psPAX2 and pMD2G with USP47 shRNA lentiviral vectors (Dharmacon Inc., Lafayette, CO, USA): shUSP47 #1 (TRCN0000007692); shUSP47 #2 (TRCN0000007693); shUSP47 #3 (TRCN0000007694); shRNA control

(RHS4080). Lentiviral particles were collected at 48 h and 72 h after transfection. USP47-shRNA or control virus was infected to DLD-1 cells with 5 μg/ml polybrene. Cells were incubated in complete growth medium with 10 μg/ml puromycine for the stable clone selection.

Immunocytochemistry

Cells were plated on chamber slides and grown in complete growth medium. After fixation with 4% paraformaldehyde solution for 15 min at room temperature, samples were incubated with 0.1% Trition X-100 (Sigma-Aldrich, St. Louis, MO, USA) in phosphate-buffered saline (PBS) and blocked with 3% bovine serum albumin (BSA). Samples were then incubated overnight at 4°C with anti-USP47, anti-E-cadherin, anti-N-cadherin, anti-Snail, anti-vimentin, and anti-phalloidin (Biotium) antibodies. After washing with PBS, samples were incubated with anti-rabbit Alexa 488- or anti-mouse Alexa 546-conjugated secondary

antibodies (Molecular Probes, Eugene, OR, USA) for 1 h at room temperature.

Immunofluorescence

Paraffin-embedded tissues were deparaffinized with xylene. For antigen retrieval, tissues were heated in a microwave oven with citrate buffer (DakoCytomation). The sections were treated with 0.2% Triton X-100 for permeabilization, then blocked with 3% BSA in PBS for 1 h. Subsequently, the sections were incubated overnight at 4°C with anti-USP47, anti-E-cadherin, anti-N-cadherin, anti-Snail, anti-vimentin, and anti-proliferating cell nuclear antigen (PCNA) antibodies and washed with PBS. Incubation with anti-rabbit or anti-mouse secondary antibodies was carried out for 1 h at room temperature. The sections were stained using Prolong Antifade with DAPI (Invitrogen).

Immunoprecipitation

After treatment, cells were collected and lysed with RIPA lysis buffer for immunoprecipitation. Following centrifugation, the supernatant was precleared with protein A agarose beads (Millipore) coupled with mouse or rabbit IgG for 1 h and then incubated with the indicated antibodies overnight at 4°C. The cells were exposed to protein A agarose beads for 4 h. The beads were washed three times with RIPA lysis buffer. The precipitates were dissolved in SDS loading buffer for western blotting.

Cell viability assay

Cells were seeded at a density of 8,000 cells/well in 48-well plates for 24 h in an incubator. One day after seeding, the cells were transfected with pcDNA3-USP47 or siUSP47 and incubated under normoxic or hypoxic conditions for 72 h. Thiazolyl blue tetrazolium bromide (Sigma-Aldrich) was then added at a final concentration of 0.5 mg/mL, and plates were

incubated for 2 h. The MTT reagent was removed, and DMSO was added to solubilize the formazan crystals formed. The absorbance per well was measured at 570 nm using a microplate reader (Bio-Rad Laboratories, Hercules, CA, USA).

Wound healing assay

Culture inserts (Ibidi) were transferred to 6-well plates. CRC cells were seeded at a density of 5×10^4 DLD-1 cells/well in the culture inserts. After 24 h, the silicon inserts were removed, and the cells were photographed under a microscope. The separate walls were closed after 24 h, and closed gap images were captured using a microscope.

Clonogenic assay

DLD-1 cells were plated in 6-well plates at a density of 200 cells/well. RPMI medium was changed every another day, and cells were incubated under normoxic or hypoxic conditions. After 7 days, the cells formed colonies. The colonies were fixed in cold methanol and stained with 0.5% crystal violet. The stained colonies were washed with PBS to remove excessive dye. Quantitative changes in clonogenicity were determined by extracting stained dye with 10% acetic acid and measuring the absorbance of the extracted dye at 570 nm.

Invasion assay

Cell invasion assays were carried out using 24-well transwell chambers (Costa) according to the manufacturer's instructions. Briefly, DLD-1 cells were plated in the upper chamber with RPMI medium without fetal bovine serum. Cells were then incubated for 24 h, and invaded cells were stained with 0.5% crystal violet for 5 min. After washing with PBS, the stained cells were counted under a microscope.

Chromatin Immunoprecipitation (ChIP)

Chromatin was pulled down using anti-Sox9 antibodies, and a DNA fragment containing the predicted sequence of the promoter region of USP47 was analyzed with RedSafe Nucleic Acid Staining Solution (Intron Biotechnology). A potential Sox9-biding site in the promoter region of USP47 was predicted using the Genomatics database system (http://www.genomatix.de/). PCR primers were as Table 3.

Animals

Ten 5-week-old male BALB/C nude mice (Orient Bio Laboratory Animal Inc.) were injected with 1.5×10^6 DLD-1 cells mixed in Matrigel (BD Biosciences) in both flanks. Tumors were monitored every 3 days. Twenty-eight days after the injection, the mice were sacrificed by asphyxiation.

Tumor volumes were calculated using the following formula: Tumor volume = length × $(\text{width})^2 \times 0.5$. Tumor tissues were collected for western blotting and immunofluorescence analysis. The protocol was approved by the Institutional Animal Care and Use Committee (IACUC) of Seoul National University (SNU-160718-1).

Statistical analysis

The results are presented as means ± standard deviations (SDs). To determine statistical significance, Student's unpaired *t*-tests were used, and differences with *P* values of less than 0.05 were considered significant.

Results

USP47 is overexpressed in CRC

The microarray data retrieved from the Cancer Genome Atlas were analyzed through the oncomine web portal (www.oncomine.org). Hong cancer analysis was performed for samples from 9 patients with CRC (Hong et al., 2010), and Kaiser cancer analysis for tissues derived from 72 patients with rectal mucinous adenocarcinoma tissues (RMA) (Kaiser et al., 2007). The results of these analyses revealed that the expression level of USP47 in tumor tissues was relatively higher than that in the surrounding normal colon tissues (NC) (Figure 5). Immunofluorescence staining of human colorectal tissue microarrays revealed that USP47 is markedly overexpressed in colorectal adenocarcinoma compared with normal colon tissues (Figure 6).

USP47 is upregulated in CRC cells under hypoxic conditions.

I also compared the mRNA and protein expression levels of USP47 in normal CCD 841 CoN and cancerous (DLD-1, HCT-116, and HT-29) CRC cells using PCR and Western blot analyses, respectively. Of the 4 representative DUBs tested, the expression of USP47 was consistently upregulated in all 3 CRC cells examined. The mRNA levels of USP24 and USP48 were also found to be increased in some CRC cells, but not as pronounced as that of USP47 (Figure 7A). The protein expression levels of USP47 in normal and cancerous colorectal cells showed similar patterns. Thus, USP47 showed consistently high expression in three different types of CRC cells, compared to CCD841 CoN normal human colon epithelial cells (Figure 7B). In contrast, the expression level of USP7 remained similar between cancerous and normal cells.

To confirm whether hypoxia directly regulates expression of USP47 and EMT markers, the aforementioned CRC cells were maintained in a 1% hypoxia chamber for 72 h. Hypoxia enhanced the expression of USP47 and representative mesenchymal markers (e.g., N-cadherin and vimentin) whereas it suppressed that of the epithelial marker, E-cadherin at

the transcriptional and translational levels (Figure 8A and B, respectively). The results of the immunocytochemical analysis were similar. Thus, N-cadherin and vimentin as well as USP7 were accumulated under hypoxia, while the level of E-cadherin was diminished (Figure 9). Collectively, these findings suggest that hypoxia upregulates the expression of USP47 and promotes EMT in DLD-1, HCT-116, and HT-29 CRC cells.

Silencing of USP47 promotes EMT in CRC cells under hypoxic conditions

To ensure that USP47 plays a crucial role in the regulation of EMT, CRC cells were transfected with siUSP47 RNA and then subjected to 1% hypoxia for 72 h. Knockdown of USP47 suppressed the expression of vimentin and N-cadherin and restored E-cadherin expression under hypoxic conditions (Figure 10). Immunofluorescence analysis verified that siUSP47 transfection reduced the expression of vimentin and N-cadherin and enhanced that of E-cadherin in hypoxia (Figure 11). During EMT, actin

cytoskeleton remodeling and focal adhesion formation occur which are associated with increased cell movement. Focal-adhesion-anchored actin stress fibers play an important role in mechano-signal transduction and cell migration (Tojkander et al., 2012). Vimentin has been suggested to regulate intracellular mechanical homeostasis by maintaining cytoskeleton architecture and the balance of cell force generation in cancer cells undergoing EMT (Liu et al 2015). In line with this notion, there was a pronounced formation of actin stress fibers and focal adhesion as visualized by staining against phalloidin (Figure 11). Moreover, the silencing of USP47 impeded manifestation of fibroblast-like morphology (Figure 12A) and also the migration of DLD-1 cells (Figure 12B). The growth of DLD-1 cells was also inhibited by silencing of USP47 in hypoxia-mimicking condition (Figure 13). In addition, the USP47 knockdown attenuated the invasiveness of DLD-1 cells (Figure 12C).

Overexpression of USP47 enhances invasiveness and metastatic potential of CRC cells

In an attempt to further verify the involvement of USP47 in hypoxia-induced EMT in CRC cells, I transfected the DLD-1 cells with USP47-pcDNA vector. Upon USP47 overexpression, the levels of N-cadherin and vimentin were increased even in normoxia, compared to those in the mock-transfected cells, whereas the expression level of E-cadherin was reduced (Figure 14A). USP47-pcDNA3-transfected DLD-1 cells exhibited shattered and fibroblast-like shapes, while the morphology of the mock transfected cells remained unchanged (Figure 14B). Immunocytochemical analysis showed the disassembly of E-cadherin and concomitant accumulation of mesenchymal marker proteins in USP47-pcDNA3-transfected DLD-1 cells (Figure 15). Overexpression of USP47 also increased the number of invasive DLD-1 cells (Figure 17A), and the migration of DLD-1 cells (Figure 17B).

USP47 binds to Snail and triggers its deubiquitination

In exploring how USP47 regulates EMT, I initially focused on Snail, a transcription factor that has a pivotal role in the regulation of EMT. DLD-1 cells in hypoxic conditions showed elevated expression of Snail as well as its mRNA transcript (Figure 17A). Transient knockdown of USP47 in DLD-1 cells lowered the expression of Snail protein. However, the mRNA expression of Snail was not affected by silencing of USP47 (Figure 17B). These finding suggest that USP47 may stabilize Snail protein by counteracting its ubiquitination.

To test the possibility of inhibition of ubiquitination and subsequent proteasomal degradation of Snail by DUB activity of USP47, I examined the physical interaction between USP47 and its possible substrate, Snail by immunoprecipitation analysis. When DLD-1 cells were maintained in normoxia for 72 h, Snail and USP47 showed a weak interaction. However, under hypoxic conditions, USP47 binding to Snail was markedly enhanced (Figure 18A). To visualize the interaction between Snail and USP47, I stained the DLD-1 cells with fluorescent probes detecting USP47 (red) and Snail (green). In normoxic conditions, USP47 and Snail were barely detectable (Figure 18B). Under hypoxia, USP47 was

accumulated predominantly in the cytosol, but the Snail was localized in both cytosol and nucleus. This observation implies that USP47 binds to Snail and removes ubiquitins from it in the cytoplasm of DLD-1 cells. When dissociated from USP47, the free Snail translocates into the nucleus (Figure 18B). In order to test above speculation, I examined total ubiquitin level and the deubiquitination activity USP47 by an immunoprecipitation analyses. The total lysates of DLD-1 cells were incubated with ubiquitin antibody. The expression level of total ubiquitin was significantly increased in siUSP47-transfected DLD-1 cells compared to siCtrl-transfected DLD-1 cells. This result indicates that USP47 suppressed ubiquitination in DLD-1 cells both in normoxia and hypoxia (Figure 19). The control- and siUSP47-transfected DLD-1 cells were treated with the proteasome inhibitor MG-132 and exposed to hypoxia for 72 h. Silencing of USP47 significantly increased the accumulation of ubiquitinated Snail (Figure 20). In another experiment, Snail and ubiquitin-flag constructs were transfected into USP47-deleted DLD-1 cells, which were then subjected to hypoxia for 72 h. Such artificial increment of Snail and ubiquitin also enhanced the deubiquitination activity of USP47 towards Snail (Figure 21). Taken

together, these results indicate that USP47 interacts directly with Snail and impedes its ubiquitination and subsequent proteasomal degradation. The stabilized Snail then migrates to nucleus and regulates the expression of genes involved in EMT in CRC cells under hypoxic conditions.

Sox9 induces expression of USP47 by binding to its promoter region under hypoxic conditions

To elucidate the mechanisms underlying hypoxia-induced upregulation of USP47, I searched for a candidate transcription factor that could bind to the promoter region of the gene encoding this enzyme under hypoxia. The Genomatix database system analysis predicted Sox family transcription factors as the most likely candidates responsible for regulating the USP47 expression. Among these, I focused on Sox9 as this transcription has been reported to be overexpressed/overactivated in CRC (Table 3) (Xia et al., 2016, Lü et al., 2008). Notably, Sox9 levels are higher in metastatic than in primary CRCs from the same patient, which appears

to account for enhanced self-renewal activity and EMT (Carrasco-Garcia et al., 2016). I also found that Sox9 showed comparatively higher mRNA expression in DLD-1, HCT-116, and HT-29 cells than in normal colorectal cells, but the expression of Sox4, another protein of the Sox family, remained unchanged (Figure 22). As USP47 was overexpressed during exposure to hypoxia, I measured the Sox9 levels under the same conditions. The protein expression of Sox9 as well as USP47 was increased in all three CRC cell lines after challenged to hypoxia for 72 h, and this accompanied the characteristic profile of EMT markers (Figure 23A). There was also a robust increase in the mRNA level of Sox9 in the same cell lines under hypoxia (Figure 20B). To investigate the association between USP47 and Sox9, DLD-1, HCT-116, and HT-29 cells were transfected with commercially available Sox9 siRNA prior to exposure to hypoxia for 72 h. The mRNA expression level of USP47 was dramatically reduced in all these Sox9 knockdown cell lines under hypoxic conditions (Figure 24A). Furthermore, the silencing of Sox9 suppressed the expression of USP47 protein and manifestation of EMT (Figure 25B).

The Genomatics database system predicted USP47 promoter segments A (-877 to -831 bp), B (-493 to -466 bp), and C (-356 to -348 bp) as potential biding sites for Sox9 (Table 4, Figure 25). To verify the specificity of these sites, I also chose non-specific sites, NS-1 and NS-2. Based on this prediction, I designed primers for Sox9 binding and examined the binding affinity of Sox9 for each primer. As illustrated in Figure 26, Sox9 interacted most strongly with the promoter segment A (-877 to -831 bp). Therefore, it is likely that hypoxia induces the expression of Sox9, which, in turn, binds to a specific site located at a position -877 to -831 bp from the transcription start site in the USP47 promoter region.

Knockdown of USP47 inhibits invasive and metastatic capabilities of colon cancer cells

Because hypoxia-induced USP47 expression enhanced EMT by stabilizing Snail, I investigated the contribution of USP47 to tumor growth and invasion *in vivo*. For long-term experiments, stable USP47 knockdown

cell lines were established using 3 commercially available shUSP47 plasmid constructs. Of the 3 established stable USP47-knockdown DLD-1 cell lines, cells transfected the shRNA construct #2, showing the lowest expression levels of USP47 (Figure 27), was chosen for the subsequent xenograft experiment.

Mock- or shUSP47 #2 treated DLD-1 cells were mixed with Matrigel and injected subcutaneously into both flanks of 4-week-old male BALB/C nude mice. The USP47 knockdown dramatically reduced the size (Figure 29), the volume (Figure 30A) and the weight (Figure 30B and C) of the tumors. The expression of Snail and EMT markers was markedly reduced in USP47-shRNA transfected DLD-1 cells, compared to the control shRNA (shCtrl) transfected DLD-1 cells (Figure 31). Tumor tissues were stained against USP47, Snail, and EMT markers for immunofluorescent analysis (Figure 32). The expression levels of USP47 and mesenchymal markers were enhanced, and E-cadherin was diminished in the shCtrl group. However, the USP47-shRNA-treated group exhibited reduced expression of mesenchymal markers with restoration of epithelial E-cadherin (Figure 44). In line with the *in vitro* findings, knockdown of USP47 abrogated the

expression of EMT markers in transplanted tumors, and this led to suppression of progression and invasiveness of CRC cells. To check metastasis capability of USP47, I injected control- and shUSP47-transfected DLD-1 cells into the tail vain of mice. After 28 days, mice were sacrificed, then lung was extracted to evaluation. Notably, knock-down of USP47 reduced the number of nodule in lung tissues compare to control (Figure 28).

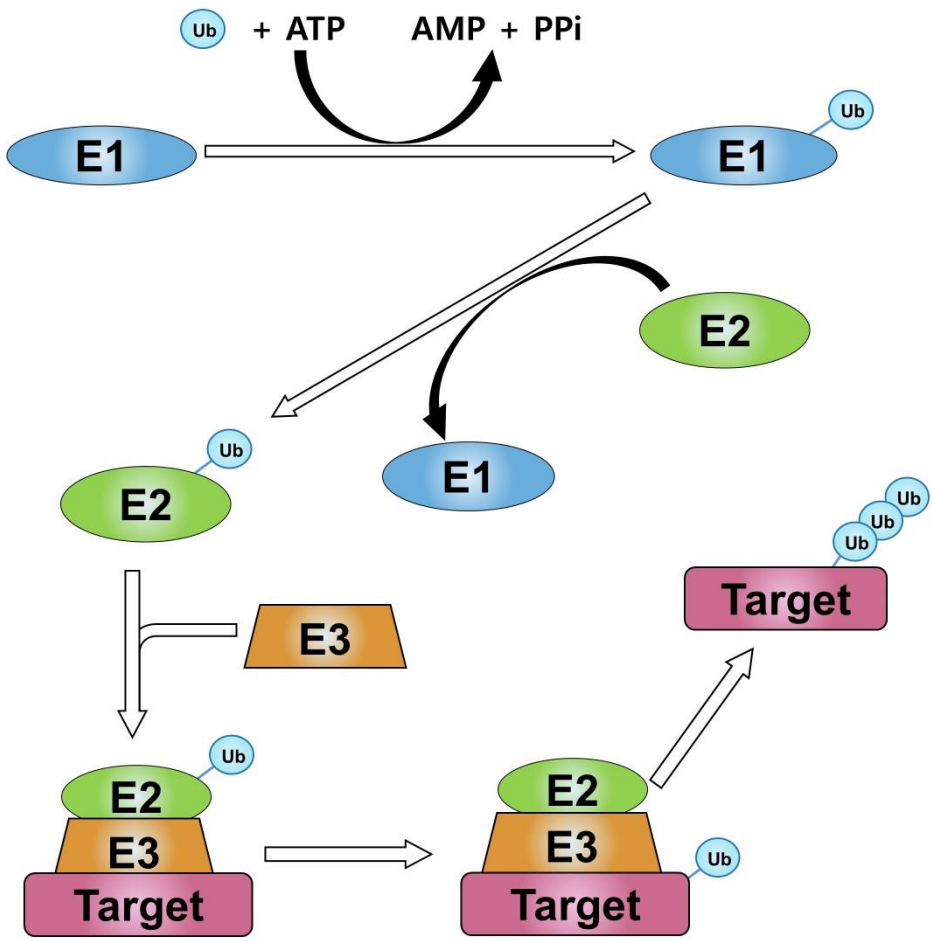

Figure 1. Ubiquitination System A schematic representation of the protein ubiquitination pathways.

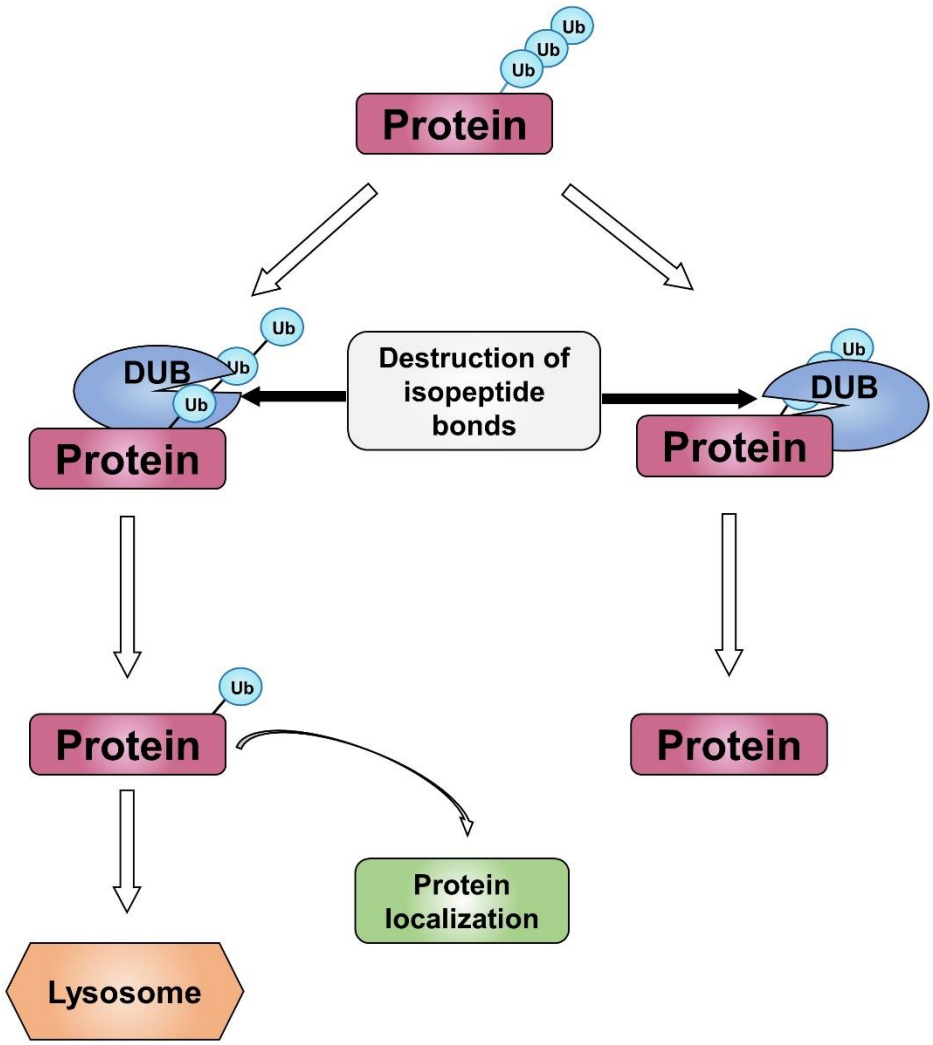

Figure 2. Deubiquitination System An overview of deubiquitination processes.

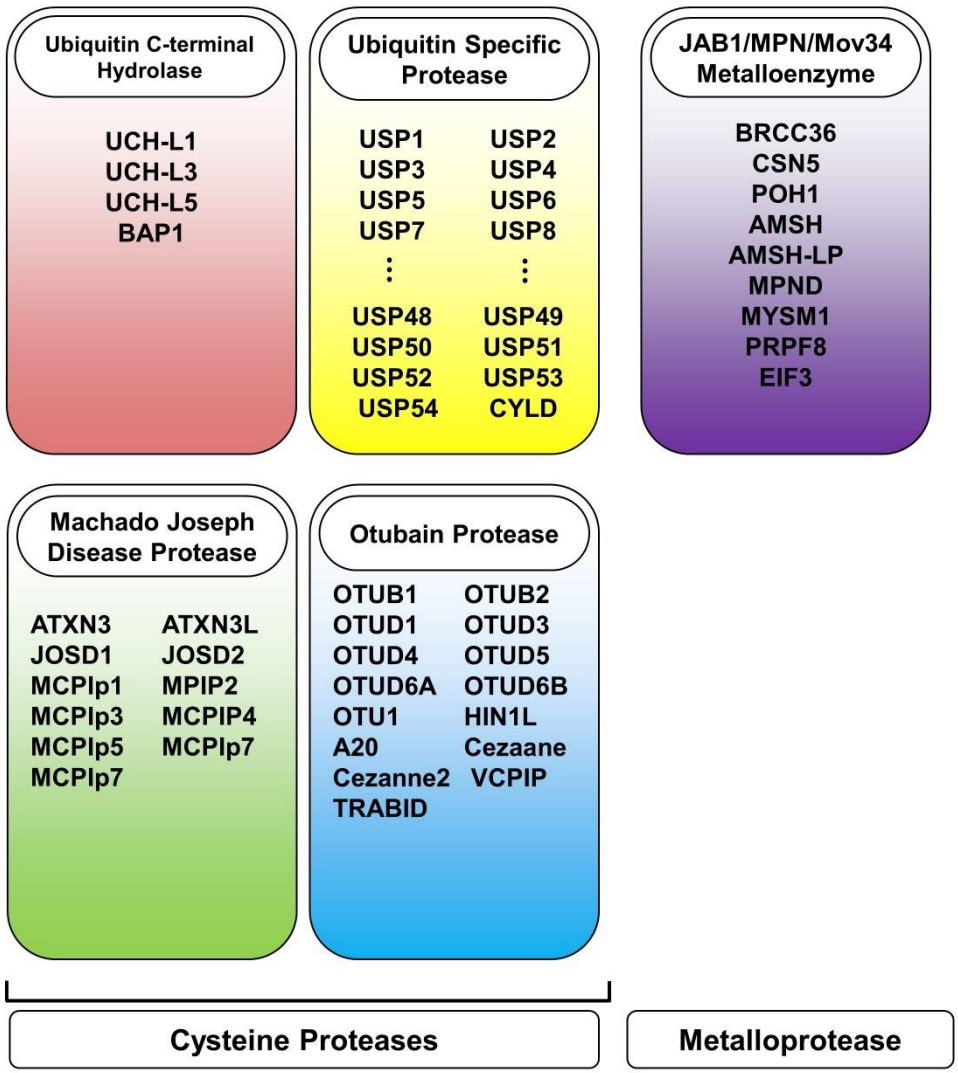

Figure 3. A family of Deubiquitinating enzymes

Name	Substrate protein	Relate signal pathway	Cancer progression	References
UCHs				
UCHL1	AKT2, HIF-1α	AKT pathways, Hypoxia	Breast cancer	Nakashima, et al., Luo, et al.
BAP1	BRCA, HCFC1	Cell growth, Cell cycle regulation.	Renal tumorigenesis, Various cancers	Jensen, et al, Misaghi, et al., Harbour, et al.,
UCHL3		Metastasis	EMT	Song, et al.
USPs				
CYLD	TRAF2/6, NEMO, Bcl3, Dvl	NF-κB, JNK and p53 Pathway, Cell death	Cylindromatosis of the scalp, colitis, hepatocellular carcinoma	Kovalenko, et al., Yoshida, et al., Jono, et al.
USP1	FANCD2, PCNA	DNA repair	Colorectal cancer	Liang et al., Dharahar, et al.
USP2a	Fatty acid synthase, RIP, TRAF2, Myc, Mdm2	Fas/p53, NF-kB, Myc, EGFR	Prostate and Breast cancer	Graner, et al., Qu, et al., Wei, et al., Liu et al.
USP3	BRCA1	DNA repair, GSTA2	Breast and Ovarian cancer	Sharma, et al., Whalen et al.
USP5	P53, FOXM1	p53, cell proliferation	Pancreatic cancer	Daya, et al., Li et al.
USP6	Unknown	Chromosomal rearrangement, WNT/-catenin pathways	Ewing's sarcoma, Aneurysmal bone cysts	Oliveira, et al., Madan, et al.

USP7	P53, FOXM1	p53, PI3-K, PTEN, FOXO4	Prostate cancer, Gliomas	Li, et al., Atanassov, et al.
USP8	EGFR, 14-3-3, FLIPS, ErbB2, HIF-1α	Cell proliferation, PTEN-AKT pathways, Hypoxia response	Lung cancer, Colon cancer	Berlin, et al, Alwan, et al, Balif, et al, Panner, et al, Troilo, et al.
USP9X	Claspin	ATR-Chk1		Mcgarry, et al.
USP10	P53 and MSH2	ATM-p53 and mismatch repair		Yuan, et al., Zhang, et al.
USP11	P53	DDR-Chk1		Ke, et al.
USP15	Mdm2, CSN9, Smurf2, TRI, SMAD2	NF-kB, Wnt pathways	Breast and ovarian tumors and Glioblastoma	Zou, et al, Schweitzer, et al, Eichhorn, et al, Ivengar et al.
USP19	HIF-1α, KPC1, IAPs, MuRF and MAFbx/atrogin-1	Hypoxia response, Apoptosis, Skeletal muscle regulation	Breast and prostate cancer	Lu, et al., Mei, et al., Bedard, et al.
USP20	pVHL,	Hypoxia response, NF-kB	Lung and Gastrointestinal cancer	Li, et al., Jean-Charles, et al., Curcio, et al., Morellli, et al.
USP28	FBW7, CHK2, 53BP1	Myc, DNA damage, Cell proliferation	non-small lung cancer, Colorectal cancer, Breast cancer	Popov, et al., Zhang, et al., Lei et al.

USP29	p53	p53, Oxidative stress		Liu, et al.
USP31	TRAF2/6, NEMO	NF-kB	Breast cancer	Li, et al.
USP33	β-arrestin	7TMR transfricking	Various of cancer	Erin, et al.
USP42	p53, PHLPP, AKT	p53, RUNX fusion gene, Cell proliferation	AML, Colorectal cancer	Hock, et al, Li et al.
USP47	SCF-TRCP, BER	G2/M Checkpoint		Shi, et al., Peschiaroli, et al.
MJDs				
ATXN3	PTEN, P53	PI3K, Cell death, Cell proliferation	Gastric cancer, lung cancer cells	Gao, et al.
ATXN3L	KLF5	Cell proliferation	Breast cancer	GE, et al.
OTUB				
OTUB1	FOXM1, RhoA, RAS, EMT, KRAS	DNA damage, Drug resistance, EMT, p53	Multiple cancer	Karunarathna, et al., Wang, et al., Iglesias-Gato, et al., Zhou, et al., Baietti, et al.
OTUD5	P53 and PDCD5	P53		Luo, et al., Park, et al.

Table 1. Functions of deubiquitinating enzymes in cancer progression

Primer	Sequence
USP47	5′-GCTTTCGGACTGGGGTAGAT-3′
	5′-AGAACCAACTGGTCCCGAAG-3′
Sox9	5′-GTGGTCCTTCTTGTGCTGC-3′
	5′-GTACCCGCACTTGCACAAC-3′
CDH1	5′-GCTGGAGATTAATCCGGACA-3′
	5′-ACCCACCTCTAAGGCCATCT-3′
CDH2	5′-ACAGTGGCCACCTACAAAGG-3′
	5′-CCGAGATGGGGTTGATAATG-3′
vimentin	5′-CTCTTCCAAACTTTTCCTCCC-3′
	5′-AGTTTCGTTGATAACCTGTCC-3′
Snail	5′-CCTCCCTGTCAGATGAGGAC-3′
	5′-CCAGGCTGAGGTATTCCTTG-3′
GAPDH	5′-ACCCAGAAGACTGTGGATGG-3′
	5′-TCTAGACGGCAGGTCAGGTC-3′

Table 2. Primer sequences

Figure 4. A schematic structure of domains in USP47 A schematic structure have been resolved for USP47 domains which has 4 different UBL domain.

USP47 gene expression in Oncomine® database

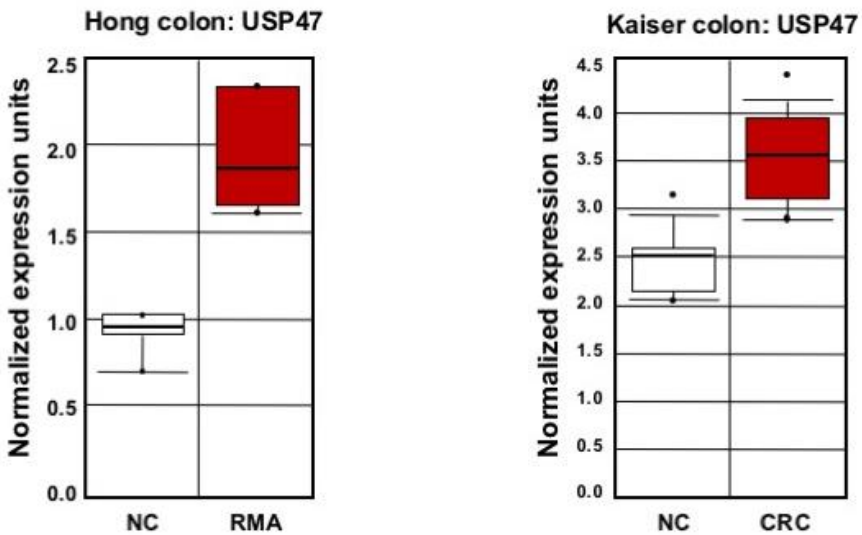

Figure. 5. Overexpression of USP47 gene expression in Oncomine® databases Association of *USP47* mRNA levels with the CRC subtype. Data obtained through Oncomine indicate that CRC tissues display higher levels of USP47 than surrounding tissues.

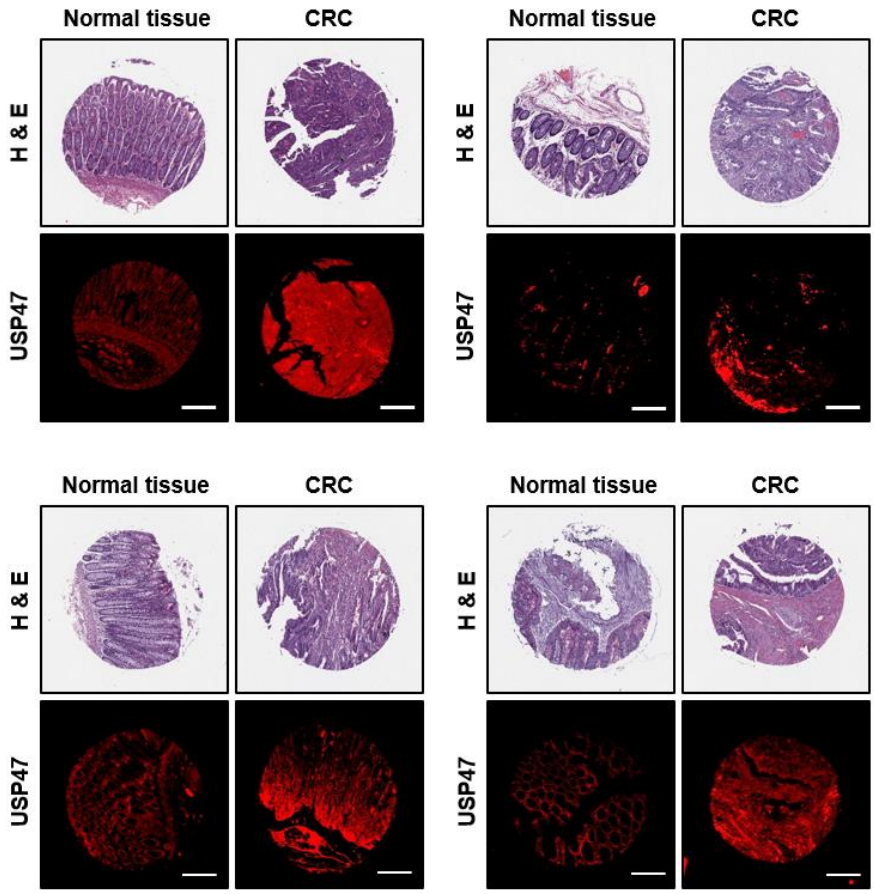

Figure 6. Overexpression of USP47 in CRC Representative immunofluorescent images for USP47 protein expression in normal and CRC tissues. Samples from a human CRC tissue microarray containing colorectal carcinoma and adjacent normal tissues were examined by immunofluorescence staining with an anti-USP47 antibody. Hematoxylin and eosin (H&E) images were provided by US Biomax Inc. Scale bar = 200 μm.

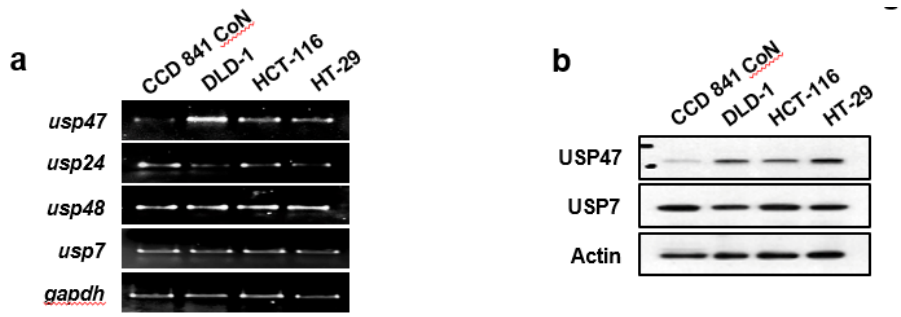

Figure 7. Overexpression of USP47 in CRC cells (**a**) and (**b**) The mRNA and protein levels of USP47 in normal colon epithelial CCD841 CoN cells and CRC (DLD-1, HCT-116, and HT-29) cells were measured by PCR (**a**) and Western blot (**b**) analyses, respectively under hypoxic conditions.

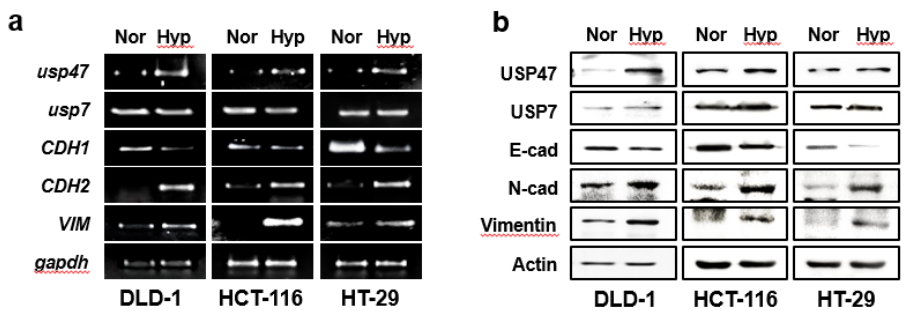

Figure 8. Elevated expression of USP47 and EMT markers in CRC cells under hypoxic condition (**a**) and (**b**) DLD-1, HCT-116, and HT-29 cells were exposed to normoxia (Nor) or hypoxia (Hyp) for 72 h, and expression of USP47, E-cadherin, N-cadherin, and vimentin at transcriptional (**a**) and translational (**b**) levels was examined by PCR and Western blot analyses, respectively.

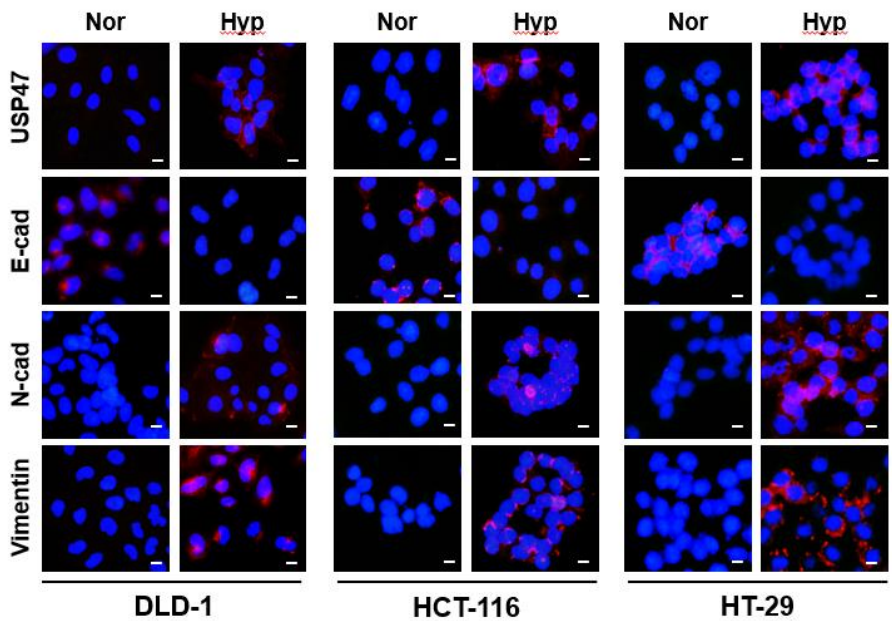

Figure 9. Hypoxia-induced USP47 and EMT markers were accumulated in CRC cells Representative confocal microscopy images of immunostained DLD-1, HCT-116, and HT-29 cells in normoxia and hypoxia. The cells were stained for detection of USP47, E-cadherin (E-cad), N-cadherin (N-cad), and vimentin. The nuclei were stained for DAPI. Scale bar = 100 μm.

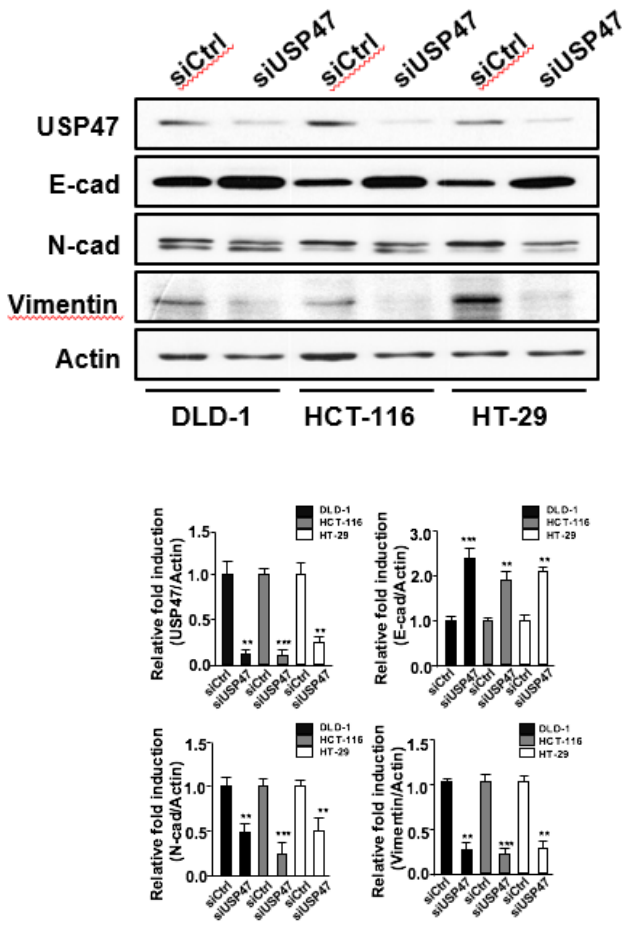

Figure 10. Protein expression of mesenchymal markers were attenuated by silencing of USP47 in CRC cells under hypoxic conditions Comparison of protein expression of USP47, E-cadherin (E-cad), N-cadherin (N-cad), and vimentin in siUSP47- or control siRNA (siCtrl)-transfected DLD-1 cells under hypoxic conditions. Protein

expression was visualized by Western blot analysis. Two-sided *t* tests were performed to assess significance; *$P < 0.05$; **$P < 0.01$.

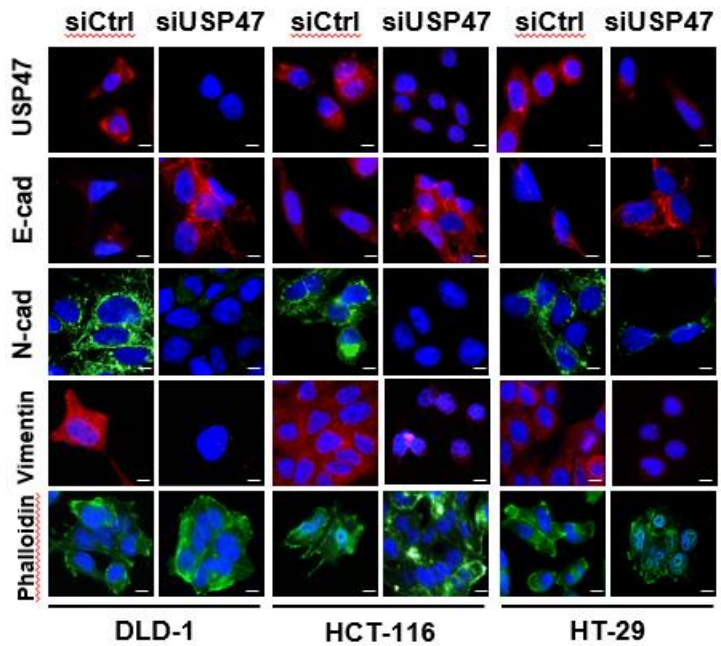

Figure 11. The silencing of USP47 reduces mesenchymal markers and recovers epithelial marker in CRC cells under hypoxic conditions

Immunocytochemical analysis of siControl- and siUSP47-transfected DLD-1, HCT-116, and HT-29 cells in hypoxia. Cells were stained for USP47, E-cad, N-cad, vimentin, and phalloidin. Scale bar = 20 μm.

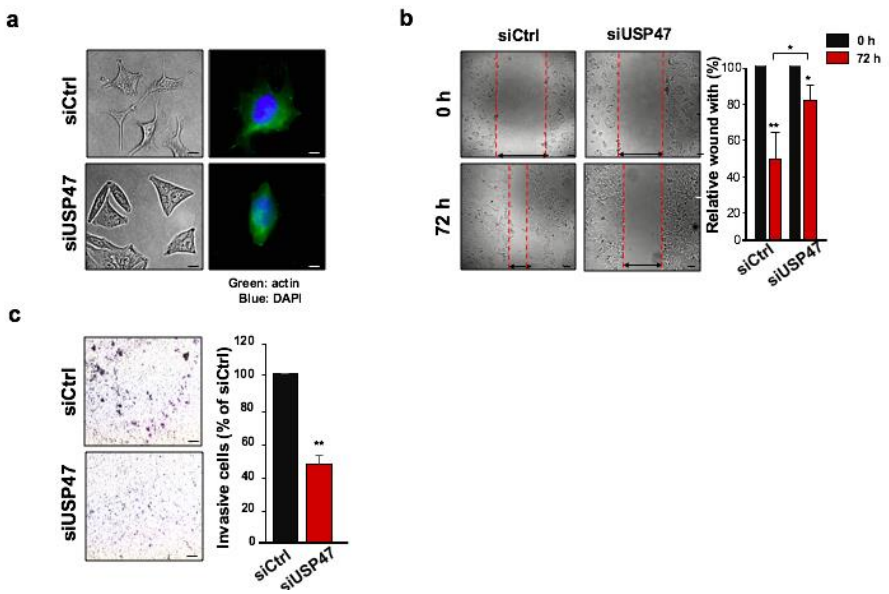

Figure 12. Attenuation of the EMT and metastatic potential by silencing of USP47 in CRC cells under hypoxic conditions (**a**) Representative photo-micrographs depicting morphological and actin cytoskeleton modification in USP47-silenced DLD-1 cells under hypoxic conditions. Cells were stained for detection of actin. Scale bar = 20 μm. (**b**) Images of wound closure of after knockdown of USP47 in DLD-1 cells under hypoxic conditions. Scale bar = 100 μm. (**c**) USP47-siliencd DLD-1

cells were subjected to trans-well invasion assays under hypoxic conditions.

Scale bar = 150 μm; *$P < 0.05$; **$P < 0.01$; ***$P < 0.001$.

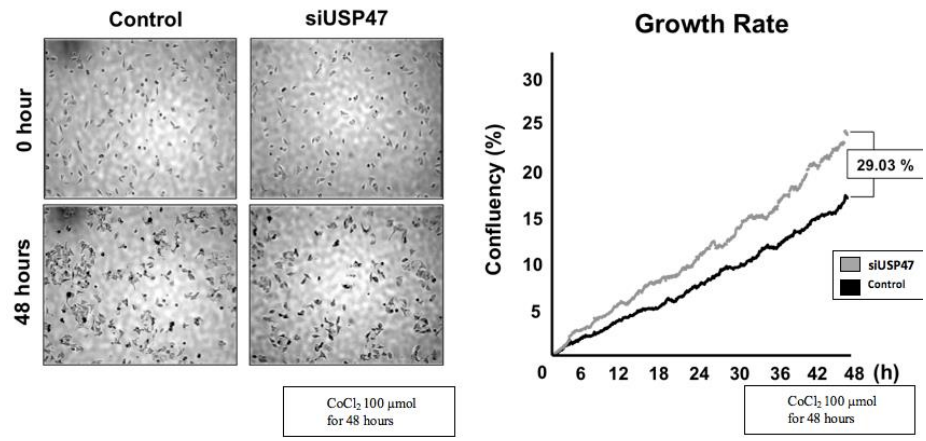

Figure 13. Silence of USP47 interferes growth of DLD-1 cells in hypoxia-mimicking situation After 48 hours of $CoCl_2$, which widely treated as hypoxia mimicking reagent, the growth rate of DLD-1 cells were decreased by silence of USP47.

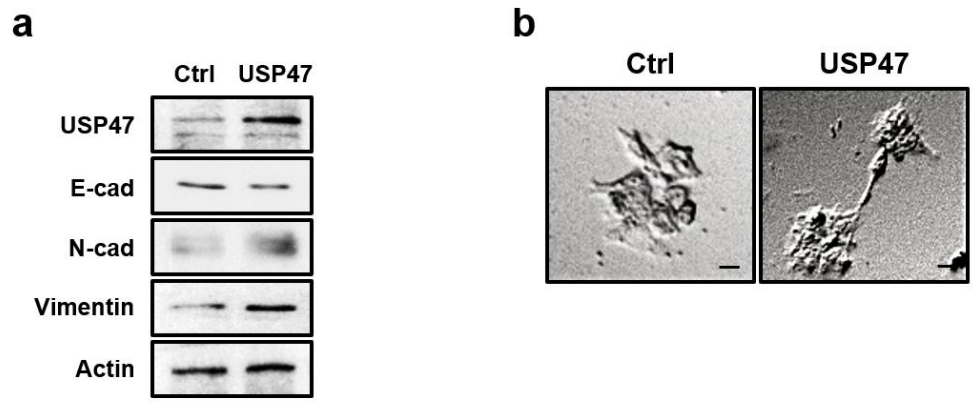

Figure 14. Enhancement of the EMT in CRC cells by USP47 overexpression under hypoxic conditions (**a**) DLD-1 cells were transfected with the pcDNA3-USP47 construct and then incubated under normoxic conditions for 72 h. Expression levels of USP47, E-cadherin, N-cadherin, and vimentin were evaluated by Western blotting. (**b**) The morphology of mock- and pcDNA3-USP47-transfected DLD-1 cells was visualized by phase contrast microscopy. Scale bar = 20 μm.

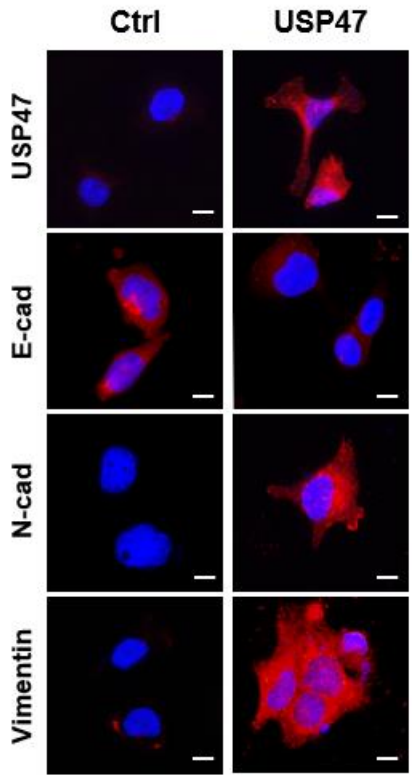

Figure 15. Overexpressed USP47 enhances accumulation of mesenchymal markers, whereas diminishes E-cadherin in normoxia

Immunocytochemical analysis of pcDNA3-USP47-transfected DLD-1 cells stained for USP47, E-cadherin, N-cadherin, and vimentin under normoxic conditions. Scale bar = 20 μm.

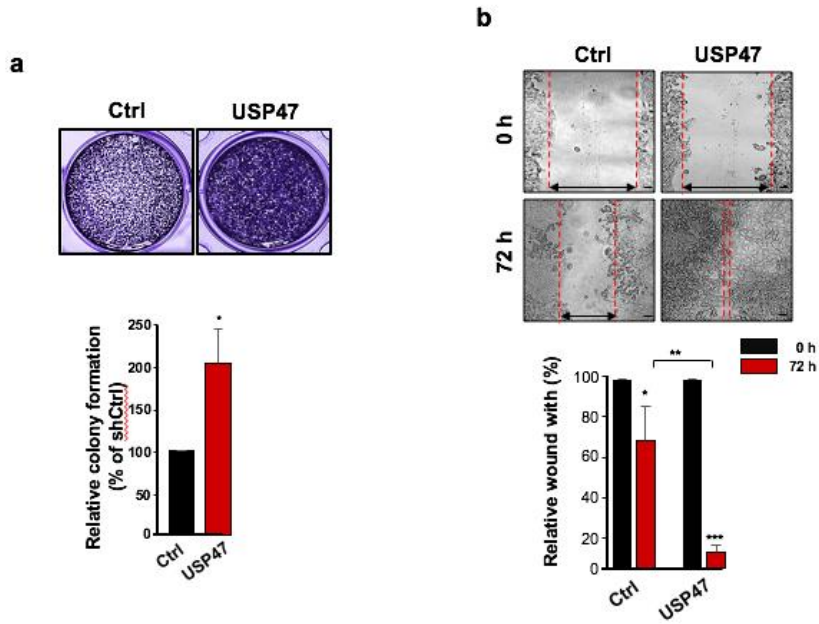

Figure 16. Enhancement of the EMT and metastatic potential by overexpression of USP47 in nomoxia (**a**) Representative images of colony formation assays in pcDNA3-USP47-transfected DLD-1 cells. Scale bar = 200 μm; **P* < 0.05. ***P* < 0.01. ****P* < 0.001. (**b**) Representative images of enhanced wound closure of pcDNA3-USP47-transfected DLD-1 cells subjected to hypoxic conditions. Scale bar = 100 μm. Results are representative of three independent experiments.

Significantly different between the groups compared; *$P < 0.05$; ***$P <$ 0.001.

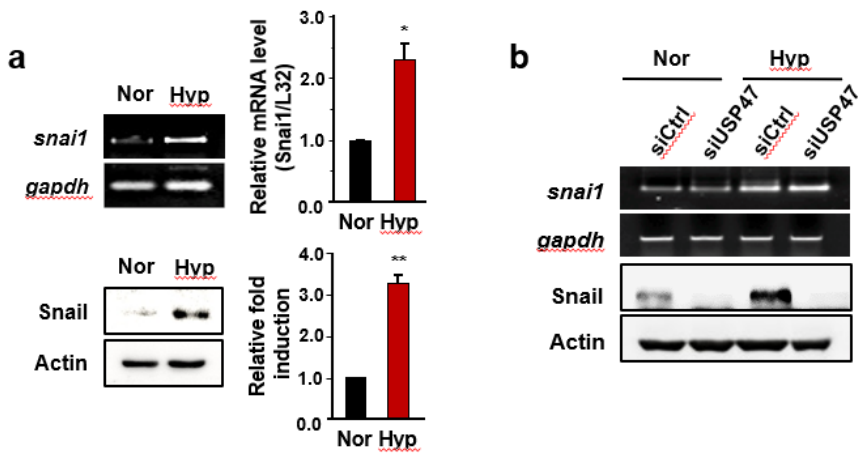

Figure 17. USP47 regulates Snail through regulating protein stability of Snail (**a**) mRNA and protein expression levels of Snail in DLD-1 cells were examined by RT-PCR and Western blot analyses, respectively. Cells were exposed to normoxia or hypoxia for 48 or 72 h. (**b**) mRNA and protein expression levels of Snail in siUSP47-transfected DLD-1 cells under normoxic and hypoxic conditions were measured by RT-PCR and Western blot analyses, respectively.

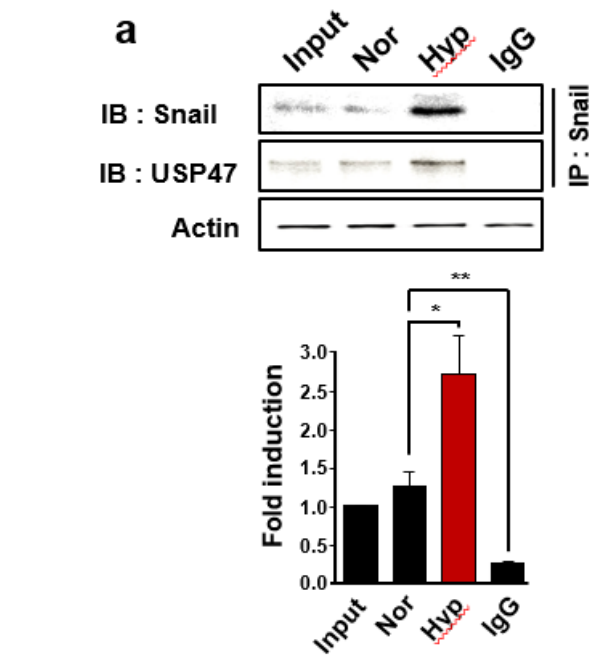
a
Input
Nor
Hyp
IgG
IB : Snail
IB : USP47
Actin
IP : Snail
**
*
Fold induction
3.0
2.5
2.0
1.5
1.0
0.5
0.0
Input
Nor
Hyp
IgG

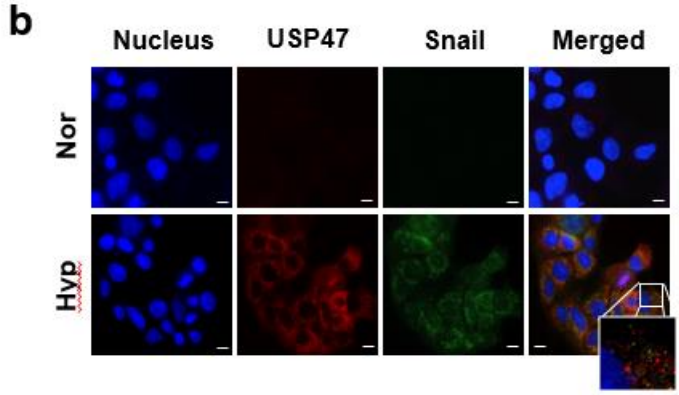
b
Nucleus
USP47
Snail
Merged
Nor
Hyp

Figure 18. USP47 physically binds to Snail in the cytosol of DLD-1 cells under hypoxic condition (**a**) Cellular lysates of DLD-1 cells were immunoprecipitated with anti-Snail and anti-USP47 antibodies, and immunoprecipitates were immunoblotted with anti-Snail antibody. (**b**) DLD-1 cells were stained for USP47 and Snail by immunocytochemical analysis. Nuclei were stained using DAPI. Scale bar = 100 μm.

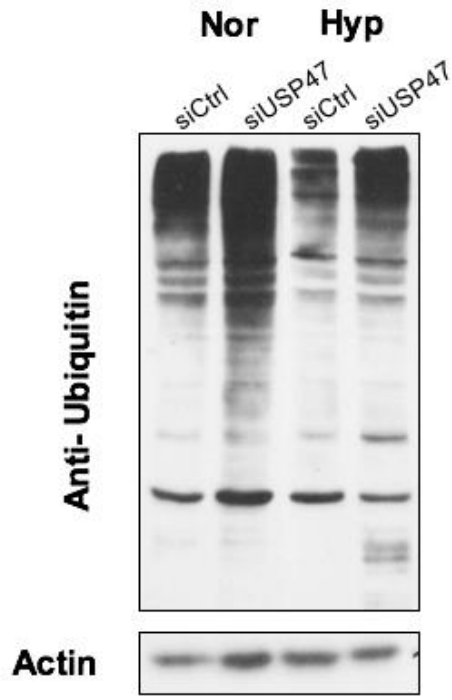

Figure 19. Silence of USP47 reduces total ubiquitination in DLD-1 in normoxia and hypoxia Total ubiquitination level was decreased accordingly the expression of USP47. Transient knock-down of USP47 notably diminishes ubiquitin expression in DLD-1 cells.

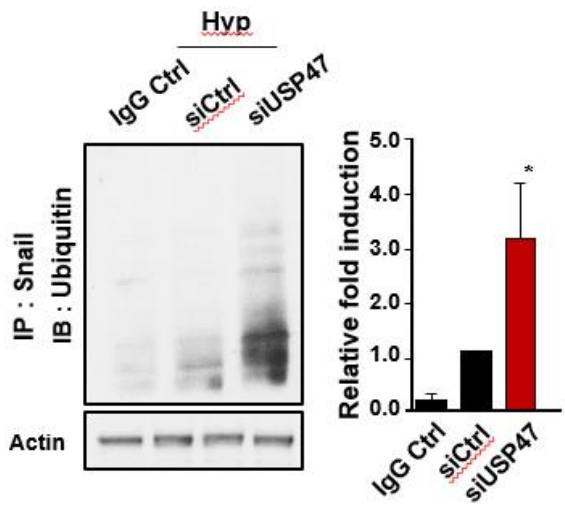

Figure 20. Stabilization of Snail by USP47 Levels of Snail-attached ubiquitins in USP47-silenced DLD-1 cells were evaluated by immunoprecipitation analysis.

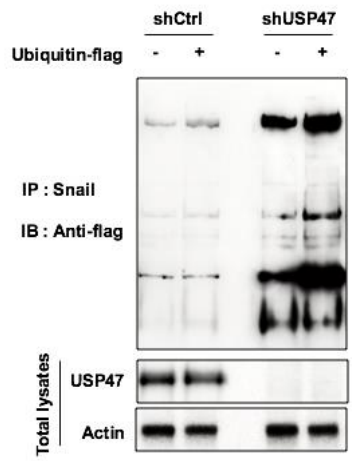

Figure 21. The expression of USP47 cleaves artificially increased ubiquitinated Snail Evaluation of ubiquitin-flag construct-transfected control and USP47-deficient DLD-1 cells. Snail immunoprecipitates were immunoblotted with anti-flag antibody. Results are representative of three independent experiments. Significantly different between the groups compared; $*P < 0.05$; $**P < 0.01$.

	Family Name	P-value	Match Total	Sequence
SOX9	Sox Family	**0.23349**	**25**	**9**
GATA2	Gata binding factors	0.02188	5	9
HIF	Hypoxia inducible factors (HIFs)	0.656923	4	4

Table 3. Sox9 was predicted as the most potential protein which can bind to promoter legion of USP47 by genomatics database system.

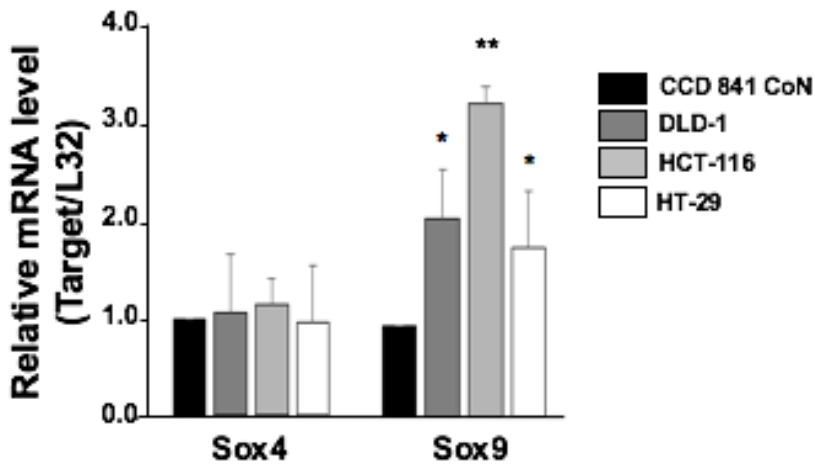

Figure 22. Sox9 is overexpressed in three different colorectal cancer cells The protein expression of Sox9 and Sox4 was evaluated by Western blot analysis in CCD 841 CoN normal colon cells and DLD-1 HCT-116, HT-29 CRC cells under nomoxic condition. Sox9 was consistently upregulated in CRC cells.

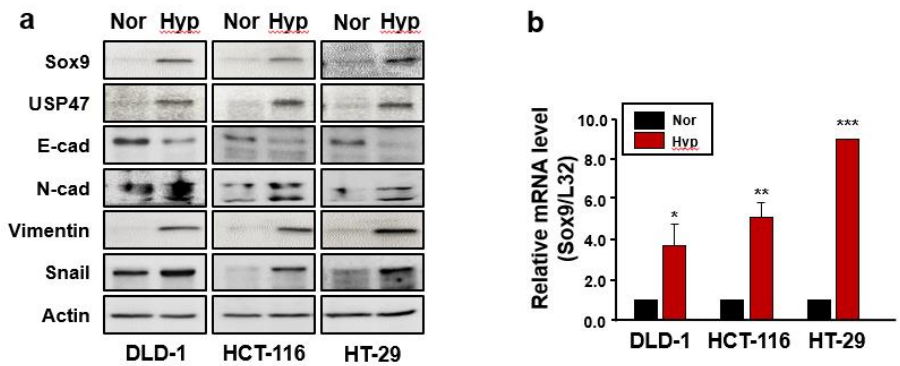

Figure 23. Hypoxia enhances expression of Sox9 (**a**) and (**b**) Effects of hypoxia on expression of Sox9 and USP47 proteins (**a**) and their mRNA transcripts (**b**) in CRC cells were assessed by Western blot and PCR analyses, respectively.

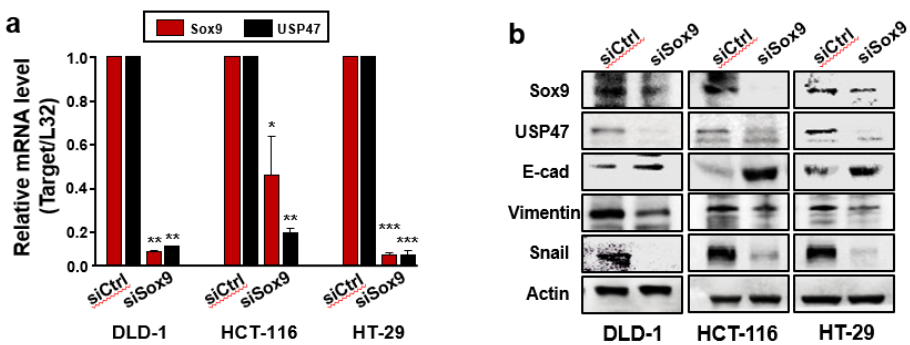

Figure 24. Sox9-mediated upregulation of USP47 expression in hypoxia (**a**) and (**b**) Cells were subjected to PCR (**a**) and Western blot (**b**) analyses to assess the expression of USP47 in siSox9-transfected CRC cells.

Primer	Sequence
Segment A	5′-GCTTATGACAGCCATTAAAACC-3′
	5′-ATACGTGTCCTGCTGTGTGC-3′
Segment B	5′-CACACAGCAGGACACGTATA-3′
	5′-ACAGTGATCTTACAGCATGCT-3′
Segment C	5′-AGCATGCTGTAAGATCACTGT-3′
	5′-CCTGTGATCTCCGTTAACAAGG-3′

Table 4. Sequence of ChIP assay

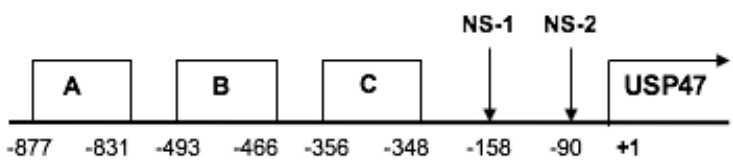

Figure 25. Sox9 directly binds to promoter legion of USP47

A Schematic diagram illustrating the position of putative Sox9 binding elements located in the promoter of human *USP47* gene.

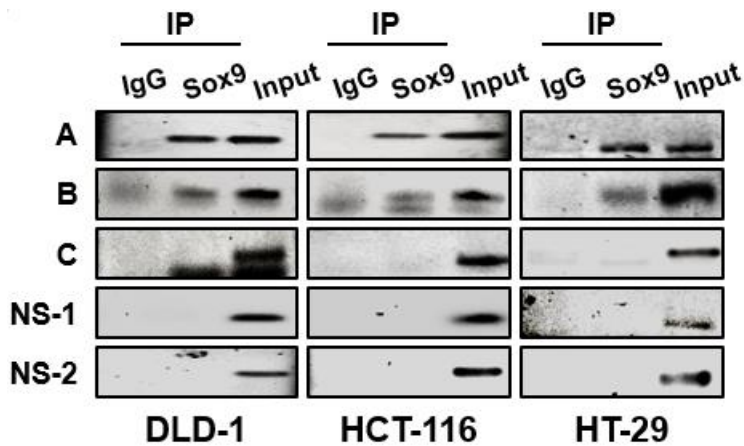

Figure 26. Direct binding of Sox9 to the USP47 promoter segment A A ChIP assay was carried out using chromatin prepared from CRC cells. The binding of Sox9 to the *USP47* promoter was detected by visualization of the PCR product. Results are representative of three independent experiments. Significantly different between the groups compared; **P* < 0.05; ***P* < 0.01.

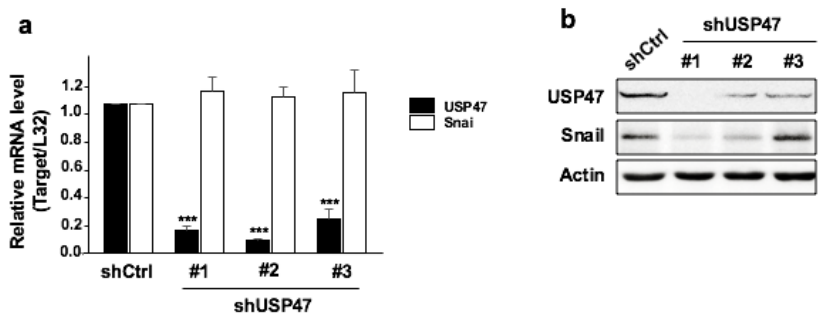

Figure 27. Establishment of shUSP47 Commercially purchased shUSP47 plasmid constructs were transfected into DLD-1 cells. mRNA and protein expression of USP47 and Snail were examined by qPCR (**a**) and Western Blotting (**b**) analyses.

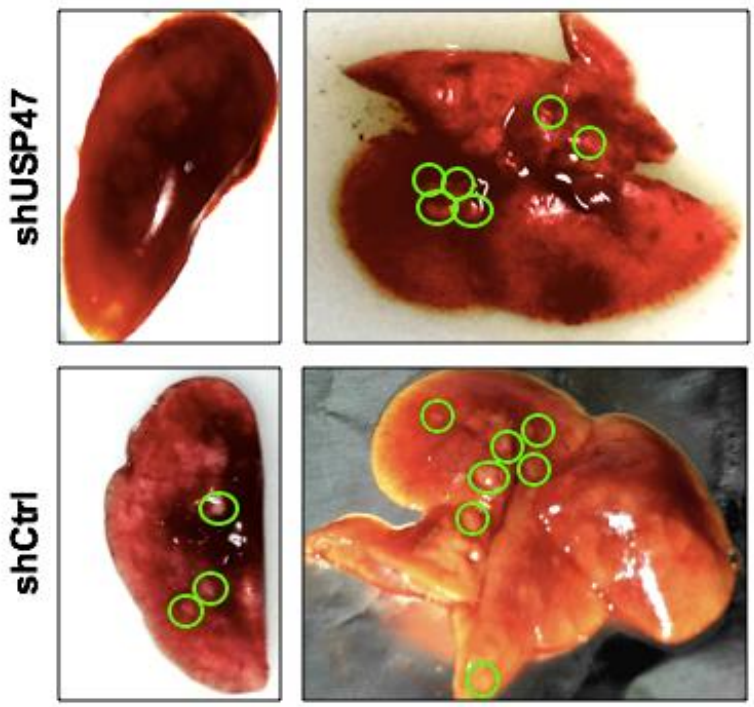

Figure 28. Knock-down of USP47 inhibits formation of nodule in lung in mice tail injection After 28 days of injection, Mice were sacrificed, and lung was extracted for evaluation. shUSP47 DLD-1 cells decreased number of nodule occurred in mice lung compare to shCtrl-transfected lung.

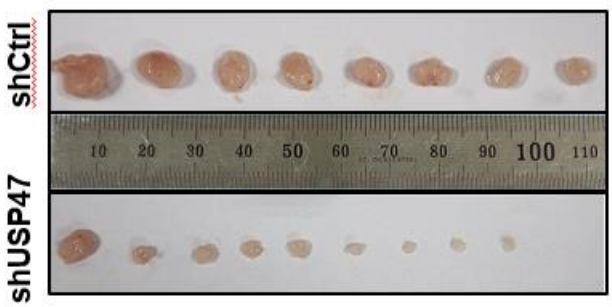

Figure 29. Inhibition of xenograft CRC tumor growth by stable knockdown of USP47 BALB/C nude mice were injected subcutaneously with shControl- or shUSP47-transfected DLD-1 cells (N = 5 mice/group) and sacrificed after 4 weeks. (**a**) Representative images of xenografts derived from shCtrl- and shUSP47-transfected DLD-1 cells.

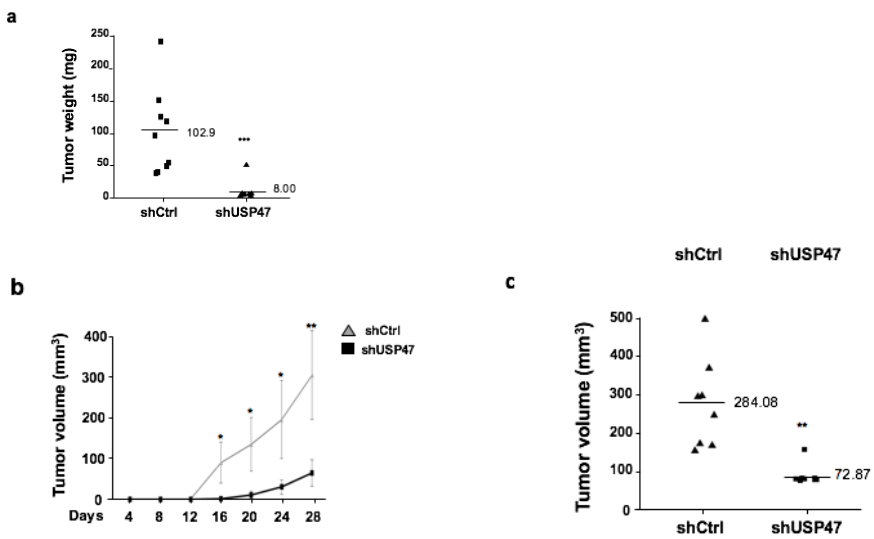

Figure 30. Size and volume of xenografted CRC tumor was reduced by shUSP47 transfection (**a**), (**b**) and (**c**) Histograms showing changes in the weight (**a**) and the weight (**b, c**) of tumors. Results are representative of three independent experiments. Significantly different between the groups compared; **P* < 0.05; ***P* < 0.01; ****P* < 0.001.

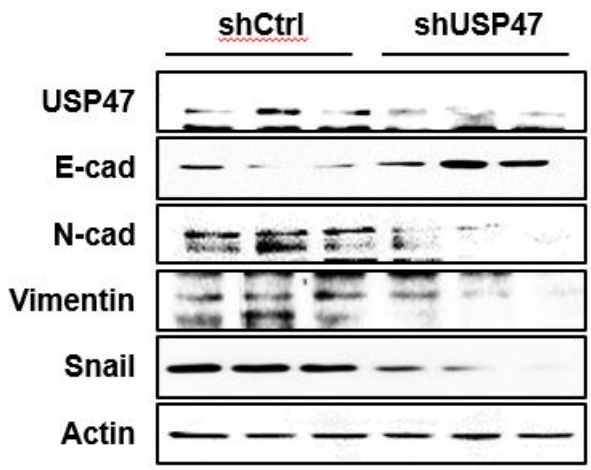

Figure 31. shUSP47 transfection inhibited EMT in xenografted tumor tissues Protein expression levels of USP47 and EMT markers in xenografts derived from USP47-deficient and control DLD-1 cells were examined by Western bolt analysis.

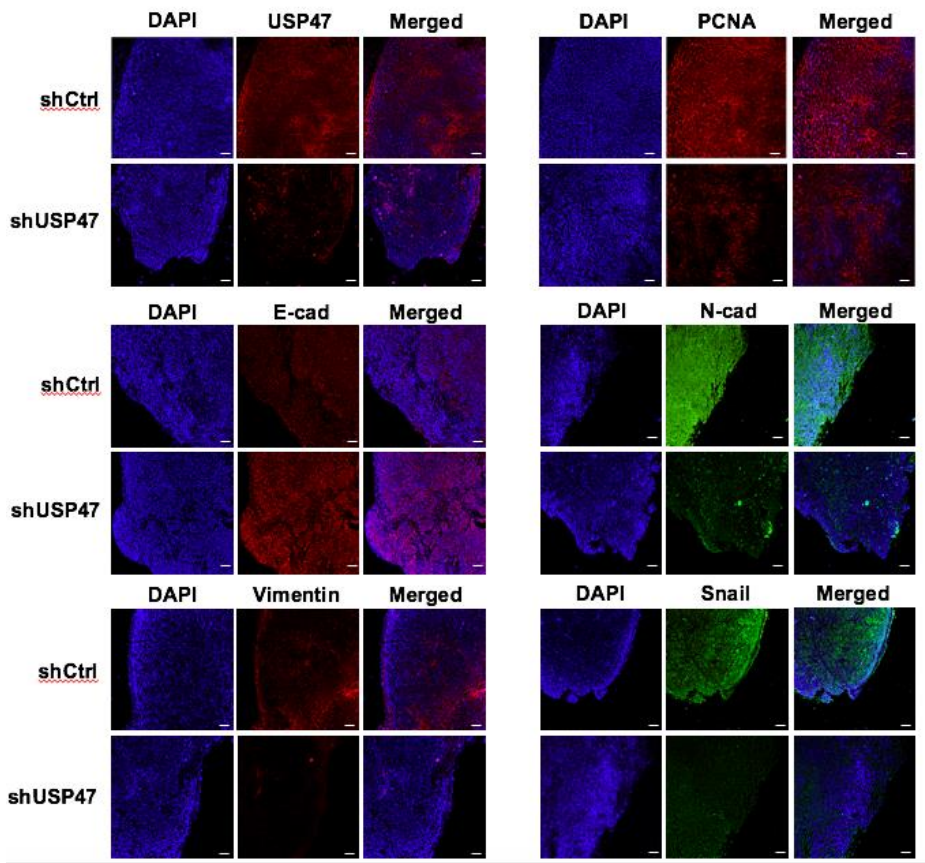

Figure 32. shUSP47 transfection enhances accumulates of mesenchymal markers, while recovers E-cadherin in xenografted tumor tissues Representative immunofluorescence images of tumors derived from shControl- or shUSP47-treated DLD-1 cells. Paraffin

sections of the tumors were stained for USP47, PCNA, E-cadherin, N-cadherin, vimentin, and Snail. Scale bar = 100 μm.

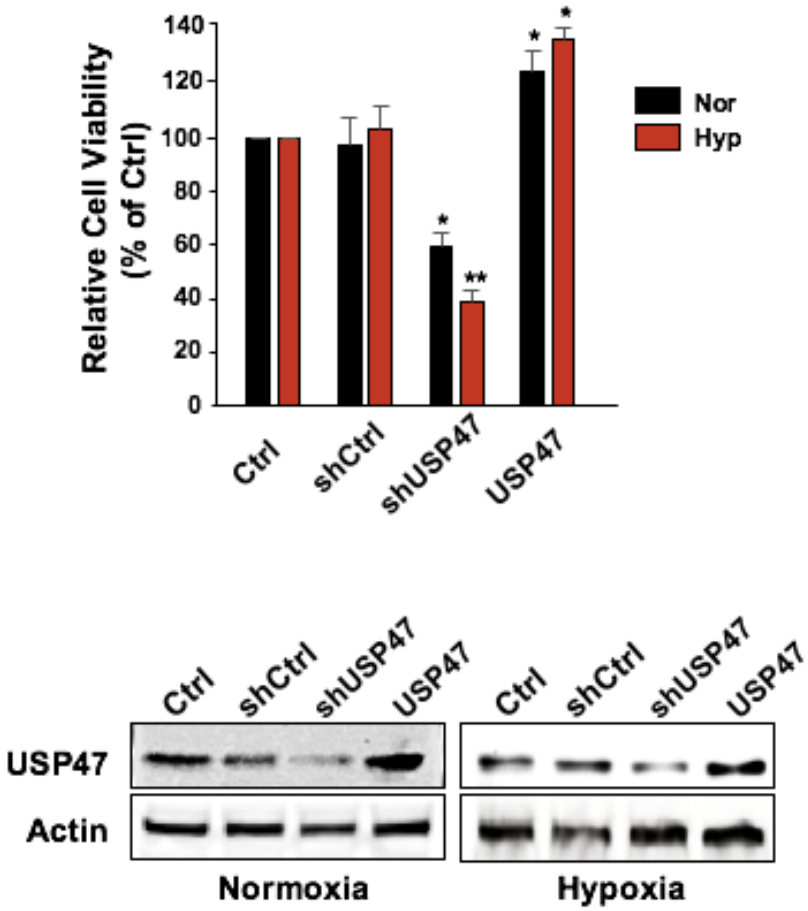

Figure 33. The growth rate of DLD-1 cells varies according to the expression level of USP47 The expression level of USP47 was regulated by transfection of shUSP47 or USP47 plasmid constructs. The growth rate of DLD-1 cells was gradually increased by USP47 increasement.

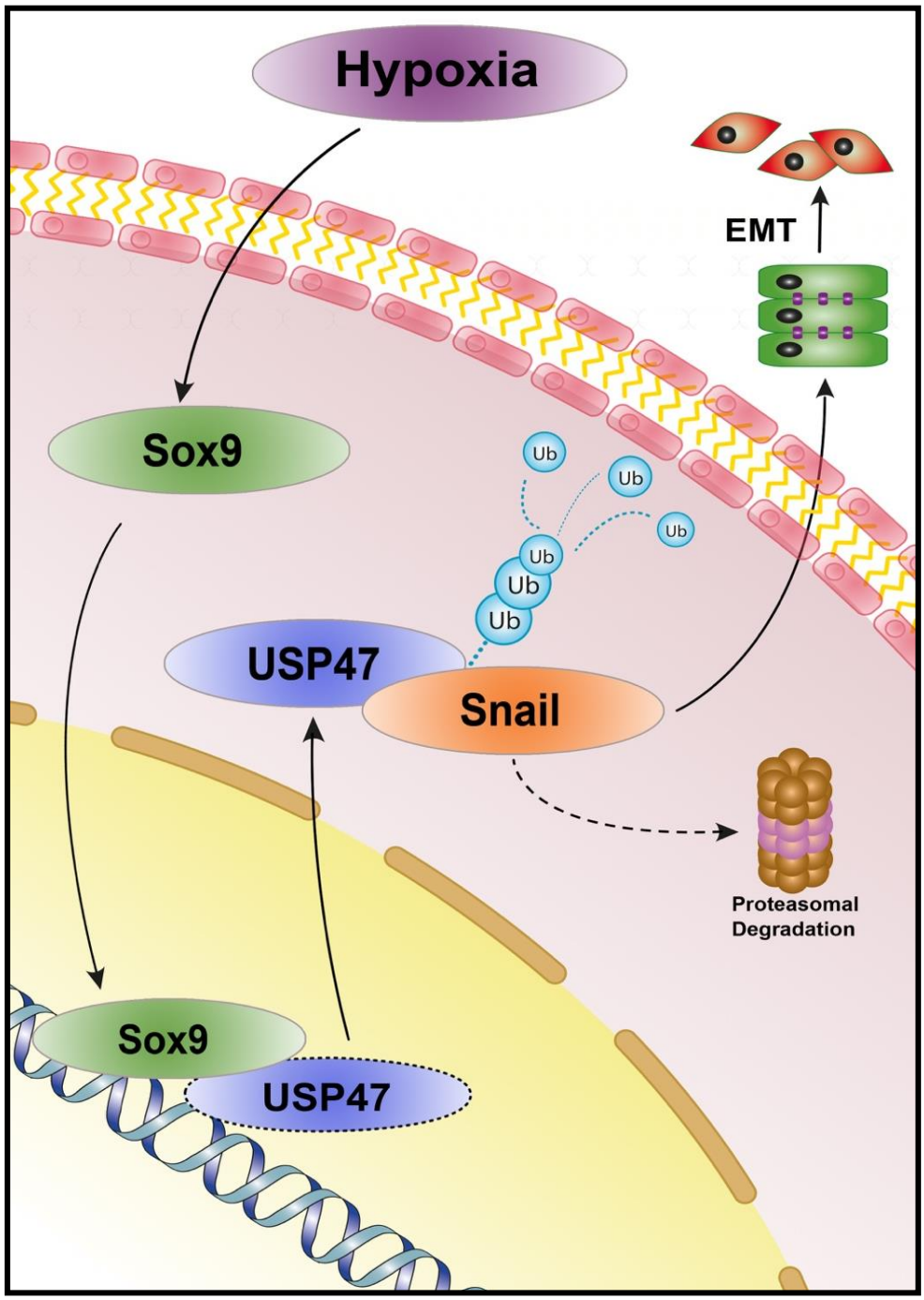
Hypoxia
EMT
Sox9
Ub
Ub
Ub
Ub
Ub
USP47
Snail
Proteasomal
Degradation
Sox9
USP47

Figure 34. A schematic representation of the USP47-mediated EMT in CRC under hypoxic conditions Hypoxia-mediated upregulation of Sox9 enhances USP47 expression which, in turn, stabilizes Snail through de-ubiquitination. Snail then translocates to nucleus where it induces the expression of proteins mediating EMT.

Discussion

DUBs, which specifically remove mono- or poly-ubiquitin chains from target proteins, regulate multiple cellular signal transduction pathways (Reyes-turcu et al., 2016). DUBs are up-regulated by various environmental and endogenous stressors. For instance, UV irradiation enhances USP24 expression, which renders damaged cells susceptible to apoptosis through p53 stabilization and PUMA activation (Zhang et al., 2016). Pro-inflammatory insults also induce expression of the specific DUB, CYLD which negatively regulates NF-κB signaling (Kovalenko et al., 2003). Like normal cells, cancer cells must survive stressful conditions. Adaptation of cancer cells to a low oxygen concentration in tumor microenvironment is essential for their growth, metabolism and angiogenesis. Such adaptive survival response of cancer cells to hypoxic conditions is mainly mediated by the transcription factor, hypoxia-induced factor-1α (HIF-1α). It has been reported that USP19 interacts with HIF-1α and thereby prevents it from degradation (Altun et al., 2012). Recently, association between dysregulated DUBs, such as USP4, -7, -11, -15, -19, -

20, -22, -36, -44, etc., and cancer has been suggested (Pfoh et al., 2015). However, the molecular basis for the possible role of USPs in cancer cell progression and metastasis is poorly understood.

In the majority of tumors, hypoxic tumor microenvironment often accompanies EMT, a process by which cancer cells become migratory and invasive. EMT occurs in most of solid cancer cells and correlates with their metastatic potential and invasiveness. Although hypoxia has been proposed to stimulate EMT, the molecular details underlying hypoxia-induced EMT remained overlooked. In order to find a novel potential signaling molecule that could contribute to hypoxia-induced EMT, I utilized the microarray database system of the Cancer Genome Atlas and identified USP47, a deubiquitinating enzyme, as a potential candidate. Notably, USP47 was found to be overexpressed in human CRC tissues as well as colon cancer cell lines. In this study, I discovered that the expression of USP47 is regulated through hypoxia-mediated Sox9 activation in CRC cells. Sox9 is a transcription factor that belongs to the High Mobility Group (HMG) superfamily involved in a multitude of developmental processes. A possible role for Sox genes in human malignancies, including CRC, has

been reported (Güro et al., 2000, Wehrli et al., 2003, Frierson et al., 2002, Katoh et al., 2002). Of the Sox family proteins, Sox9 has been shown to be overexpressed in some invasive and metastatic human breast carcinoma (Chakravarty et al., 2011), recurrent human prostate cancer (Wang et al., 2007), and CRC (Xia et al., 2016, Lü et al., 2008, Carrasco-Garcia et al., 2016), which was associated with poor clinical outcome. Moreover, overexpressed Sox9 was found to regulate the expression of genes that encode EMT markers, such as E-cadherin, N-cadherin, and vimentin (Liu et al., 2015). Our data demonstrate that hypoxic exposure of CRC cells significantly increased the expression of Sox9 and that Sox9 binds to the promoter region of *USP47*. To the best of our knowledge, this is the first identification of a key transcription factor involved in USP47 upregulation in hypoxia.

The hypoxia-induced upregulation or transactivation of Sox9 has also been reported by other investigators. Thus, hypoxia induced Sox9 gene promoter activity as well as nuclear accumulation of HIF-1α in ST2 murine stromal cells (Robins et al., 2005). Sox9 promoter harbors putative hypoxic response element (HRE) binding sites, and elimination of a cluster of HIF

binding sequences through deletion or site-directed mutagenesis abolished the Sox9 promoter activity (Robins et al., 2005). Sox9 has been considered as a master regulator of chondrogenesis. Under hypoxic conditions, *Sox9* expression was elevated compared to that in normoxia, and this increment was lost in the HIF-1α -depleted cells (Amarilio et al., 2007). Contrary to this observation, HIF-2α, but not HIF-1α, was found to be essential for hypoxic induction of Sox9 overexpression in human articular chondrocytes (Lafont et al., 2008). I noticed that HIF-1α and HIF-2α were co-expressed at a detectable level in CRC cells exposed to hypoxia (data not shown), so it would be challenging to determine which isoform mainly regulates Sox9 upregulation in these cells.

Sox9 and Snail appear to act cooperatively with each other. Snail1 or Snail2 (Slug), in the presence of Sox9, is sufficient to induce an EMT in neural epithelial cells (Cheung et al., 2005). It has been speculated that Sox9 can directly bind to Snail (Sakai et al., 2006). During tumor progression in a murine model of prostate cancer, there was an increase in EMT-associated *Sox9* expression and changes in the Wnt/ β-catenin signaling pathway (Acevedo et al., 2007). This was also verified in human

prostate cancer cells (Sakai et al., 2006). Snail is a highly unstable protein with a short half-life and rapidly degraded by proteasomes in the cytosol (Yook et al., 2006). The stability of Snail is a mainly regulated by GSK-3β, a kinase located downstream of the PI3K/Akt or the Wnt/ β-catenin signaling pathway (Mishara et al., 2010, Wang et al., 2013). NF-κB also has been found to inhibit ubiquitination of Snail, through COP9 singalosome2 (Wu et al., 2009). I found that the USP47 elevated the protein level of Snail without influencing the expression of its mRNA. Notably, USP47 interacts directly with Snail and enhances its stability. Consequently, stabilized Snail translocates to nucleus and functions as a regulator of EMT in CRC cells. The Snail protein has conserved motifs, Snail1/GFI (SNAG) and four zinc finger domains in N-terminal and C-terminal regions, respectively (Wang et al., 2013). The SNAG motif has a role in regulating Snail protein stability (Lin et al., 2010). It has been reported that SNAG motif is responsible for interaction of Snail with Dub3, a member of USP subfamily (Wu et al., 2017). The zinc finger domain of Snail is known to function as a nuclear localization signal (Yamasaki et al., 2005). However, DUBs that interact with a zinc finger domain of Snail have not been

identified yet. It has been reported that the zinc finger domain of COP9 sinalosome is essential for binding to USP15 (Hetfeld et al., 2005). It would be worthwhile determining whether USP47 can bind to Snail at the SNAG or zinc finger domains and whether such interaction contributes to stabilization of its substarte Snail.

The results from our present study provide convincing evidence that USP47 could regulate the growth of CRC cells through distinct mechanisms. When USP47 expression was blocked, the viability, migration, and invasiveness of DLD-1 cells was suppressed. In contrast, when USP47 was overexpressed in DLD-1 cells, the cell viability was significantly increased, compared to the mock control group (Figure 30). USP47 stabilizes Snail, which promotes cancer progression by blocking TGF-β-induced apoptosis (Franco et al., 2010). Knockdown of Snail has been shown to significantly inhibit tumor growth and metastasis by enhancing tumor-infiltrating lymphocytes and the systemic immune response (Kudo-Saito et al., 2009). Moreover, overexpression of POL-β, which is stabilized by USP47 in CHO/AA8 cells, enhances the growth of carcinomas in immune deficient mouse (Bergoglio et al., 2002). All these

findings, together with results from our present study, supports the oncogenic function of USP47.

In summary, the exposure of CRC cells to hypoxic conditions significantly increased the expression of Sox9. Sox9 then migrates to the nucleus and upregulates the expression of USP47, which hampers the ubiquitination of Snail, thereby preventing the proteasomal degradation of Snail (Figure 34). Our finding of USP47 as a novel regulator of Snail in hypoxia-mediated EMT of CRC cells provides a new therapeutic and prognostic option targeting this DUB.

References

Babita M, Matthew PW, Robert Y, Laura Q, Kelly AO, Meagan R, et al, USP6 oncogene promotes Wnt signaling by deubiquitylating Frizzleds. *PNAS*, 2016;**113**(21):E2945-E2954

Oliveira AM, His BL, Weremowicz S, Rosenberg AE, Dal Cin P, Joseph N, Bridge JA, et al., USP6 (Tre2) fusion oncogenes in aneurysmal bone cyst. *Cancer Res*, 2004;**64**(6):1920-3

Song HM, Lee JE, Kim JH, Ubiquitin C-terminal hydrolase-L3 regulates EMT process and cancer metastasis in prostate cell lines. *Biochem Biophys Res Commun*, 2014;**452**(3):722-7

Jean-Charles P-Y, Zhang L, Wu J-H, Han S-O, Brian L, Freedman N, et al., Ubiquitin-specific protease 20 regulates the reciprocal functions of β-arestin2 in toll-like receptor 4-promoted nuclear factor κB (NF-κB) activation. *J Bio Chem,* 2016;**291**(14):7450-64

Curcio-Morelli C, Zavacki Am, Christofollete M, Gereben B, de Freitas BC, Harney JW, et al., Deubiquitination of type 2 iodothyronine deiodinase by von Hippel-Lindau protein interacting deubiquitinating enzymes regulates thyroid hormone activation. *J Clin Invest,* 2003;**112**(2):189-96

Wang J-H, Wei W, Guo, Z-X, Shi M, Guo R-P, Decreased cezanne expression is associated with the progression and poor prognosis in hepatocellular carcinoma. *J Transl Med,* 2015;13;41.

Wang Y, Zhou X, Xu M, Weng W, Zhang, Q Yang Y, et al., OTUB1-catalyzed deubiquitination of FOXM1 facilitates tumor progression and predicts a poor prognosis in ovarian cancer. *Oncotarget*, 2016;**7**;36681-36697.

Baietti MF, Simicek M, Abbasi Asbagh L, Radaelli E, Lievens S, Crowther J, et al., OTUB1 triggers lung cancer development by inhibiting RAS mono-ubiquitination. *EMBO Mol Med*, 2016;**8**;3;288-303.

Zhou Y, Wu J, Fu X, Du W, Zhou L, Meng X, Yu H, et al., OTUB1 promotes metastasis and serves as a marker of poor prognosis in colorectal cancer, *Mol Cancer*. 2014;**28**;13:258.

Iglesias-Gato D, Chuan, Y-C, Jiang N, Svensson C, Bao J, Paul I, et al., OTUB1 de-ubiquitinating enzyme promotes prostate cancer cell invasion *in vitro* and tumorigenesis *in vivo*, *Molecular Cancer*. 2015;**14**:88.

Karunarathna U, Kongsema M, Zona S, Gong C, Cabrera E, Gomes A R, et al., OTUB1 inhibits the ubiquitination and degradation of FOXM1 in Breast cancer and eprubicin resistance, *Oncogene*. 2015;**35**;1433-1444.

Patterson-Fortin J, Shao G, Bretscher H, Messick T, Greenberg RA, Differential regulation of JAMM domain deubiquitinating enzyme activity within the RAP80 complex, *J Biol Chem*. 2010;**285**(40)30971-81

Gao R, Liu Y, Silva-Fernandes A, Fang X, Paulucci-Holthauzen A, Chatterjee A, et al., Inactivation of PNKP by Mutant ATXN3 triggers apoptosis by activating the DNA damage-response pathway in SCA3, *PloS Gene*. 2015;11;**1**:e1004834.

Hershko A, Ciechanover A. The ubiquitin system. *Annu Rev Biochem*. 1998;**67**;425–79.

Hicke L. Protein regulation by monoubiquitin. *Nat Rev Mol Cell Biol*. 2001;**2**;195–201.

Stewart B, Wild, C.P. (eds.), International Agency for Research on Cancer, WHO. World Cancer Report 2014. 2014.

Cancer incidence and mortality worldwide: sources, methods and major patterns in GLOBOCAN 2012. 2015. Ferlay J, Soerjomataram I, Dikshit R, Eser S, Mathers C, Rebelo M, et al. Cancer incidence and mortality worldwide: sources, methods and major patterns in GLOBOCAN 2012. *International journal of cancer*, 2015; **136**; E359-E386.

SEER*Explorer: An interactive website for SEER cancer statistics [Internet]. Beta Version. Surveillance Research Program, National Cancer Institute. [Cited 2017 Apr 14]. Available from https://seer.cancer.gov/explorer/

Eccles SA, Welch DR. Metastasis: recent discoveries and novel treatment strategies. *The Lancet* 2007; **369**: 1742–1757.

Weiss L. Metastatic Inefficiency. *Advances in cancer research*, 1990; **54** :159–211.1

Gout S, Huot J. Role of Cancer Microenvironment in Metastasis: Focus on Colon Cancer. *Cancer Microenvironment* 2008; **1**: 69–83.

Yilmaz M, Christofori G. EMT, the cytoskeleton, and cancer cell invasion. *Cancer Metastasis Rev* 2009; **28**: 15–33.

Finger EC, Giaccia AJ. Hypoxia, inflammation, and the tumor microenvironment in metastatic disease. *Cancer Metastasis Rev* 2010; **29**: 285–293.

Bao B, Azmi AS, Ali S, Ahmad A, Li Y, Banerjee S *et al.* The biological kinship of hypoxia with CSC and EMT and their relationship with deregulated expression of miRNAs and tumor aggressiveness. *Biochimica et Biophysica Acta (BBA) - Reviews on Cancer* 2012; **1826**: 272–296.

Imai T, Horiuchi A, Wang C, Oka K, Ohira S, Nikaido T, *et al*. Hypoxia attenuates the expression of E-cadherin via up-regulation of SNAIL in ovarian carcinoma cells. *The American journal of pathology* 2003; **163.4**: 1437-1447.

Kudo-Saito C, Shirako H, Takeuchi T, Kawakami Y. Cancer metastasis is accelerated through immunosuppression during Snail-induced EMT of cancer cells. *Cancer cell* 2009; **15**: 195-206.

Kim YH, Kim G, Kwon CI, Kim JW, Park PW, Hahm KB. TWIST1 and SNAI1 as markers of poor prognosis in human colorectal cancer are associated with the expression of ALDH1 and TGF-β1. *Oncology reports* 2014; **31**; 1380-1388.

Wilkinson KD Regulation of ubiquitin-dependent processes by deubiquitinating enzymes. *The FASEB Journal* 1997; **11**, 1245-1256.

Peschiaroli A, Skaar JR, Pagano M, Melino G. The ubiquitin-specific protease USP47 is a novel β-TRCP interactor regulating cell survival. *Oncogene* 2010; **29**: 1384–93.

Iwanaga A, Ouchida M, Miyazaki K, Hori K, Mukai T. Functional mutation of DNA polymerase β found in human gastric cancer–inability of the base excision repair in vitro. *Mutation Research/DNA Repair* 1999; **435**: 121-128.

Wang L, Patel U, Ghosh L, Banerjee S. DNA polymerase β mutations in human colorectal cancer. *Cancer Research* 1992; **52**: 4824-4827.

Bhattacharyya N, Chen HC, Comhair S, Erzurum SC, Banerjee S. Variant forms of DNA polymerase beta in primary lung carcinomas. *DNA and cell biology* 1999; **18**: 549-554.

Shi J, Liu Y, Xu X, Zhang W, Yu T, Jia J, *et al*. Deubiquitinase USP47/UBP64E regulates β-catenin ubiquitination and degradation and plays a positive role in WNT signaling. *Mol Cell Biol* 2015; **35**: 3301–3311.

Hong Y, Downey T, Eu KW, Cheah PY. A 'metastasis-prone' signature for early-stage mismatch-repair proficient sporadic colorectal cancer patients and its implications for possible therapeutics. *Clin Exp Metastasis* 2010; **27**: 83–90.

Kaiser S, Park YK, Franklin JL, Halberg RB, Yu M, Jessen WJ, *et al*. Transcriptional recapitulation and subversion of embryonic colon development by mouse colon tumor models and human colon cancer. *Genome Biol* 2007; **8**: R131.

Tojkander S, Gateva G, Lappalainen P. Actin stress fibers–assembly, dynamics and biological roles. *J Cell Sci* 2012; **125**: 1855-1864.

Liu CY, Lin HH, Tang MJ, Wang YK. Vimentin contributes to epithelial-mesenchymal transition cancer cell mechanics by mediating cytoskeletal organization and focal adhesion maturation. *Oncotarget* 2015; **6**: 15966-15983.

Xia S, Yang Z, Qi X, Pu Y, Liu Y, Wang B, *et al.* Overexpression of SOX9 and DNMT1 predicts poor prognosis and chemoresistance of colorectal cancer. *International journal of clinical and experimental pathology* 2016; **9**: 589-600.

Lü B, Fang Y, Xu J, Wang L, Xu F, Xu E, *et al*. Analysis of SOX9 expression in colorectal cancer. *American journal of clinical pathology* 2008; **130**: 897-904.

Carrasco-Garcia E, Lopez L, Aldaz P, Arevalo S, Aldaregia J, Egaña L, *et al*. SOX9-regulated cell plasticity in colorectal metastasis is attenuated by rapamycin. *Scientific Reports* 2016; ***6***.

Reyes-Turcu FE, Ventii KH, Wilkinson KD, Regulation and cellular roles of ubiquitin-specific deubiquitinating enzymes. *Ann Rev Biochem* 2009; **78**: 363–97.

Zhang L, Gong F. Involvement of USP24 in the DNA damage response. *Molecular & Cellular Oncology* 2016; **3**: e1011888.

Kovalenko A, Chable-Bessia C, Cantarella G, Israël A, Wallach D, Courtois G. The tumour suppressor CYLD negatively regulates NF-κB signalling by deubiquitination. *Nature* 2003; **424**: 801-805.

Altun M, Zhao, B, Velasco, K, Liu H, Hassink G, Paschke J, *et al*. Ubiquitin-specific protease 19 (USP19) regulates hypoxia-inducible factor 1α (HIF-1α) during hypoxia. *Journal of Biological Chemistry* 2012; **287**: 1962-1969.

Pfoh R, Lacdao IK, Saridakis V. Deubiquitinases and the new therapeutic opportunities offered to cancer. *Endocrine-related cancer* 2015; **22**: T35-T54.

Güre AO, Stockert E, Scanlan MJ, Keresztes RS, Jäger D, Altorki, NK. Serological identification of embryonic neural proteins as highly immunogenic tumor antigens in small cell lung cancer. *Proceedings of the National Academy of Sciences* 2000; **97**: 4198-4203.

Wehrli BM, Huang W, De Crombrugghe B, Ayala AG, Czerniak B. Sox9, a master regulator of chondrogenesis, distinguishes mesenchymal chondrosarcoma from other small blue round cell tumors. *Human pathology* 2003; **34**: 263-269.

Frierson HF, El-Naggar AK, Welsh JB, Sapinoso LM, Su AI, Cheng J, *et al*. Large scale molecular analysis identifies genes with altered expression

in salivary adenoid cystic carcinoma. *The American journal of pathology* 2002; **161**: 1315-1323.

Katoh M. Expression of human SOX7 in normal tissues and tumors. *International journal of molecular medicine* 2002; **9**: 363-368.

Chakravarty G, Moroz K, Makridakis NM, Lloyd SA, Galvez SE, Canavello PR, *et al*. Prognostic significance of cytoplasmic SOX9 in invasive ductal carcinoma and metastatic breast cancer. *Experimental Biology and Medicine* 2011; **236**: 145-155.

Wang H, McKnight NC, Zhang T, Lu ML, Balk SP, Yuan X. SOX9 is expressed in normal prostate basal cells and regulates androgen receptor expression in prostate cancer cells. *Cancer research* 2007; **67**: 528-536.

Liu H, Liu, Z, Jiang, B, Peng, R, Ma, Z, Lu, J. SOX9 overexpression promotes glioma metastasis via Wnt/β-catenin signaling. *Cell biochemistry and biophysics* 2015; 73: 205-212.

Robins JC, Akeno N, Mukherjee A, Dalal RR, Aronow BJ, Koopman P, Clemens TL. Hypoxia induces chondrocyte-specific gene expression in mesenchymal cells in association with transcriptional activation of Sox9. *Bone* 2005; **37**: 313-322.

Amarilio R, Viukov SV, Sharir A, Eshkar-Oren I, Johnson S, Zelzer E. HIF1α regulation of Sox9 is necessary to maintain differentiation of hypoxic prechondrogenic cells during early skeletogenesis. *Development* 2007; **134**: 3917-3928.

Lafont JE, Talma S, Hopfgarten C, Murphy CL. Hypoxia promotes the differentiated human articular chondrocyte phenotype through SOX9-dependent and-independent pathways. *Journal of Biological Chemistry* 2008; **283**: 4778-4786.

Cheung M, Chaboissier MC, Mynett A, Hirst E, Schedl A, Briscoe J. The transcriptional control of trunk neural crest induction, survival, and delamination. *Developmental cell* 2005; **8**: 179-192.

Sakai D, Suzuki T, Osumi N, Wakamatsu Y. Cooperative action of Sox9, Snail2 and PKA signaling in early neural crest development. *Development* 2006; **133**: 1323-1333.

Acevedo VD, Gangula RD, Freeman KW, Li R, Zhang Y, Wang F, *et al*. Inducible FGFR-1 activation leads to irreversible prostate adenocarcinoma and an epithelial-to-mesenchymal transition. *Cancer cell* 2007; **12**: 559-571.

Yook JI, Li XY, Ota I, Hu C, Kim HS, Kim NH, *et al*. A Wnt–Axin2–GSK3β cascade regulates Snail1 activity in breast cancer cells. *Nature cell biology* 2006; **8**: 1398-1406.

Mishra P, Senthivinayagam S, Rana A, Rana B. Glycogen Synthase Kinase-3beta regulates Snail and beta-catenin during gastrin-induced migration of gastric cancer cells. *Journal of molecular signaling* 2010; **5**: 9.

Wang H, Wang HS, Zhou BH, Li CL, Zhang F, Wang XF, *et al*. (2013). Epithelial–mesenchymal transition (EMT) induced by TNF-α requires AKT/GSK-3β-mediated stabilization of snail in colorectal cancer. *PloS one* 2013; **8**: e56664.

Wu Y, Deng J, Rychahou PG, Qiu S, Evers BM, Zhou BP. Stabilization of snail by NF-κB is required for inflammation-induced cell migration and invasion. *Cancer cell* 2009; **15**: 416-428.

Wang Y, Shi J, Chai K, Ying X, P Zhou B. The role of Snail in EMT and tumorigenesis. *Current cancer drug targets* 2013; **13**: 963-972.

Lin Y, Wu Y, Li J, Dong C, Ye X, Chi YI, *et al*. The SNAG domain of Snail1 functions as a molecular hook for recruiting lysine-specific demethylase 1. *The EMBO journal* 2010; **29**: 1803-1816.

Wu Y, Wang Y, Lin Y, Liu Y, Wang Y, Jia J, *et al.* Dub3 inhibition suppresses breast cancer invasion and metastasis by promoting Snail1 degradation. *Nature Communications* 2017*,* **8**.

Yamasaki H, Sekimoto T, Ohkubo T, Douchi T, Nagata Y, Ozawa M, *et al.* Zinc finger domain of Snail functions as a nuclear localization signal for importin β-mediated nuclear import pathway. *Genes to Cells* 2005; **10**: 455-464.

Hetfeld BK, Helfrich A, Kapelari B, Scheel H, Hofmann K, Guterman A, *et al.* The zinc finger of the CSN-associated deubiquitinating enzyme USP15 is essential to rescue the E3 ligase Rbx1. *Current biology* 2005; **15**: 1217-1221.

Franco DL, Mainez J, Vega S, Sancho P, Murillo M, Frutos CA, *et al*. Snail1 suppresses TGF-β-induced apoptosis and is sufficient to trigger EMT in hepatocytes. *J Cell Sci* 2010; **123**: 3467–3477.

Bergoglio V, Pillaire MJ, Lacroix-Triki M, Raynaud-Messina B, Canitrot Y, Bieth A, *et al*. Deregulated DNA polymerase β induces chromosome instability and tumorigenesis. *Cancer research* 2002; **62**(12): 3511-3514

Soncini C, Berdo I, Draetta G. Ras-GAP SH3 domain binding protein (G3BP) is a modulator of USP10, a novel human ubiquitin specific protease. Oncogene 2001; 20: 3869-79.

Cohen M, Stutz F, Belgareh N, Haguenauer-Tsapis R, Dargemont C. Ubp3 requires a cofactor, Bre5, to specifically de-ubiquitinate the COPII protein, Sec23. Nat Cell Biol 2003; 5: 661-7.

Yuan J, Luo K, Zhang L, Cheville JC, Lou Z. USP10 regulates p53 localization and stability by deubiquitinating p53. Cell 2010; 140: 384-96.

Draker R, Sarcinella E, Cheung P. USP10 deubiquitylates the histone variant H2A.Z and both are required for androgen receptormediated gene activation. Nucleic Acids Res 2011; 39: 3529-42.

Liu J, Xia H, Kim M, et al. Beclin1 controls the levels of p53 by regulating the deubiquiting enzyemes

Zhang XY, Pfeiffer HK, Thorne AW, McMahon SB. USP22, an hSAGA subunit and potential cancer stem cell marker, reverses the polycomb-catalyzed ubiquitylation of histone H2A. Cell Cycle 2008; 7: 1522-4.

국문 초록

저산소 상태에 의해 유도된 대장암 세포의 상피간엽이행 촉진 과정에서 USP47 의 역할

유비퀴틴은 특정 단백질과 결합하여 단백질의 분해 과정을 유도하는 단백질이다. 유비퀴틴이 단백질에 부착되는 과정을 유비퀴틴화 (Ubiquitination) 이라고 하는데, 이 과정에서 유비퀴틴은 단백질의 프로테아좀 분해 뿐만 아니라 전사 조절, endocytosis 와 lysosomal 을 향한 단백질의 수송 (Trafficking), 카이네즈 신호 전달 등 또한 조절하는 것으로 알려져 있다. 유비퀴틴에 의한 프로테아좀 분해는 유비퀴틴 활성화 효소를

통해 ATP 를 사용하여 유비퀴틴을 활성화시키는 E1 단계와 high-energy thiol ester 를 형성하여 E3 enzyme 에 전달하는 Ubiquitin-conjugation enzyme 이 관여하는 E2 단계, 그리고 유비퀴틴 기질과 결합시키는 Ubiquitin ligase 가 관여하는 E3 로 나눠진다. 각 단계를 거쳐 단일 혹은 복수의 유비퀴틴은 대상 단백질의 라이신 잔기와 주로 결합을 하게 되고, 이 표지를 프로테아좀이 인식하여 단백질을 분해한다. 유비퀴틴을 통한 프로테아좀 분해 과정은 세포내 단백질 분해의 약 80 %를 담당하는 것으로 알려져 있다.

탈유비퀴틴화 효소 (DUBs)는 이 유비퀴틴화를 억제하는 효소들로, mono- 혹은 poly- 유비퀴틴이 표지된 특정한 단백질을 인지하여 결합한 후, 유비퀴틴과의 결합을 제거하여

단백질을 분해를 막는 역할을 주로 수행한다. 유비퀴틴화를 통한 단백질 분해는 Lysosome 을 통한 분해에 비해 정교한 시간적 조절이나 특정 기질에 대한 선택성이 높기 때문에, 이 과정을 선택적으로 조절할 수 있는 탈유비퀴틴화 효소들은 최근 많은 주목을 받고 있다. 특히, 과학자들은 탈유비퀴틴화를 조절하여 유비퀴틴이 담당하는 수 많은 세포내 반응 중에서 필요한 반응만을 선택적으로 조절하기 위하여 수많은 연구를 수행하고 있다.

본 연구에서, 탈유비퀴틴화 효소인 USP47 가 저산소에서 유래된 EMT 현상을 조절하는 역할을 한다는 것을 확인하였다. 상피간엽이행 (Epithelial-mesenchymal transition, EMT) 현상은 카데린 (cadherin)을 통한 세포와 세포간 접착을 분해하고

극적인 세포 골격의 재구성을 통해 세포가 혈관이나 림프관을 통해 일차 종양에서 벗어날 수 있는 전이 및 침식 능력을 획득할 수 있도록 한다. 다수의 종양에서 EMT 에 의한 암의 전이는 저산소, 저혈당 등을 통해 촉진된다. 이중 저산소 상태를 통한 EMT 는 지속적으로 연구되고 있지만, 아직까지 세포 내 분자 신호 기전에 관한 연구는 미흡하다.

본 연구에서 저산소 종양미세환경 아래서 EMT 를 촉진하는 세포 내 신호전달체계를 규명하기 위해, Cancer Genome Atlas 데이터베이스 시스템을 활용하여 탈유비퀴틴화 효소인 USP47 가 저산소 상태의 EMT 의 잠재적 매개체임을 확인하였다. 인간 대장암 조직의 면역형광염색실험에서 USP47 가 정상 대장 조직에 비해 대장암 조직에서 더 높게 발현되어 있는 것을

확인하였다. 또한 저산소 상태에 노출되었을 때 3 종의 서로 다른 대장암 세포 (DLD-1, HCT-116 및 HT-29)에서 USP47 의 발현이 증가하는 것을 확인하였다. 저산소 상태에서 결장암 세포의 USP47 의 증가는 Snail 를 탈유비퀴틴화하여 E-cadherin 의 분해를 유도하고 EMT 를 촉진시켰다. USP47 유전자를 억제하였을 경우 Snail 의 프로테아좀 분해를 촉진하였을 뿐만 아니라, 대장암세포에서 EMT 를 억제하여 침윤과 전이 능력도 억제하였다. 더욱이 우리는 저산소 상태를 통해 유도된 USP47 의 증가가 Sox9 를 통한 것임을 밝혔다. 즉, 저산소 상태에서 Sox9 에 의해 증가하는 USP47 이 EMT 와 암 세포의 전이를 조절한다는 것을 규명하였다. 이상의 결과는

향후 대장암 진단 및 치료를 위한 새로운 표적 물질로서 USP47 활용될 수 있음을 시사한다.

주요어

USP47, colorectal cancer, Snail, epithelial-mesenchymal transition, Sox9

학번

2007-21873